

Direct Reactions

for



*Some ideas from Task 10: Physics and Instrumentation.
Leader: Roger Page, Liverpool.*

Introduction by
Wolfgang Mittig.
Abano Terme
Town Meeting
2002

Table of direct reactions(1)

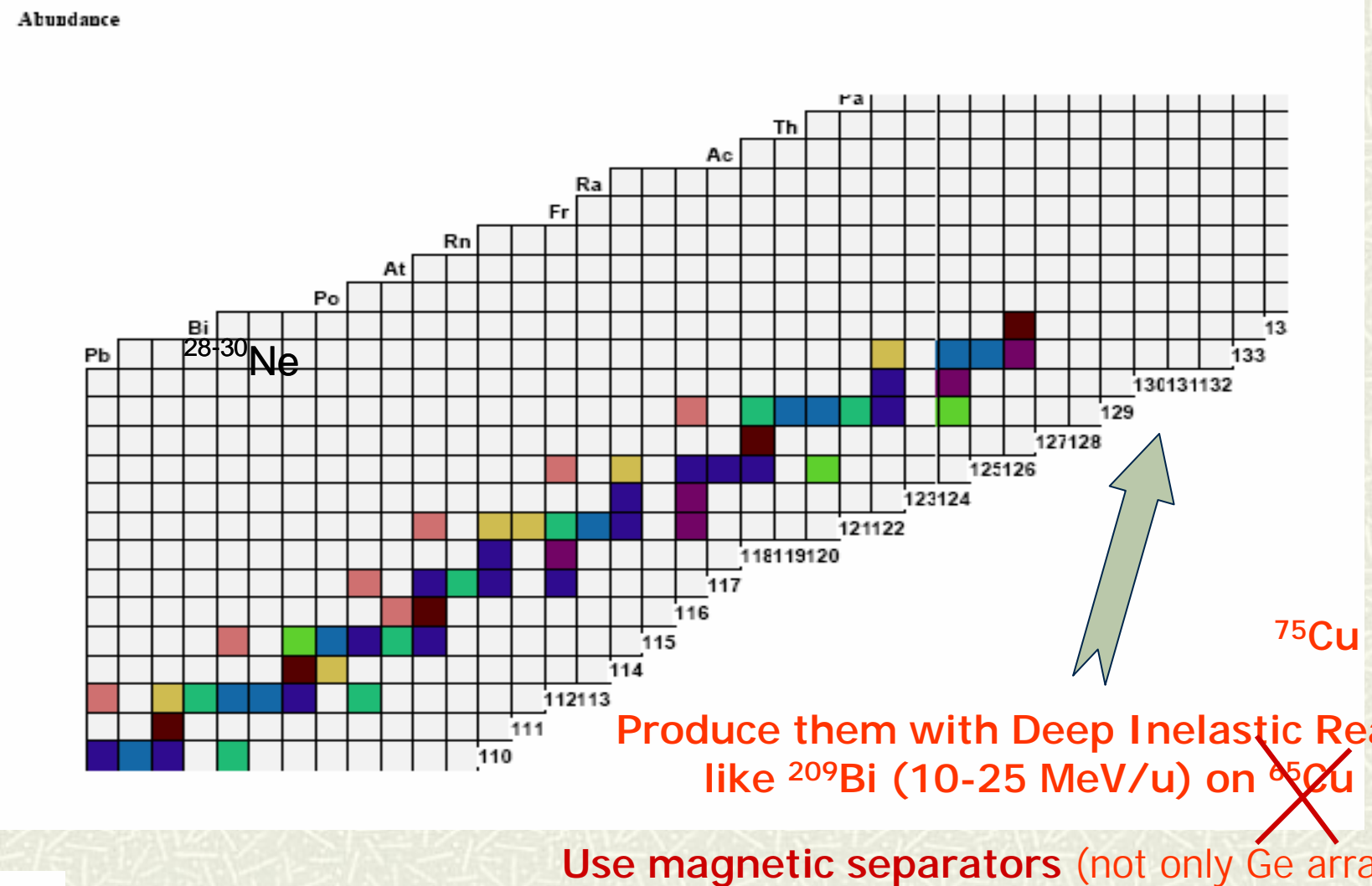
reaction	physics	target	Energy [MeV/n]	Intensity [1/s]
Elastic scattering	Interaction potentiel	p,He,C, p...	4-100	1000
	matter distribution	p,He, p	>100	10000
Inelastic scattering (Coulomb excitation)	Transition strength, deformation, collectivity, Q-moments	Pb	<5	10000
		Pb	>20	10
(nuclear inelastic)	Collectivity, 2+ states, 3-, 0+,...	p,d,He,...	>20	10
(giant resonances, dipole T=1)	Low lying dipole modes	p,He,C, Pb	>50	1000
Giant Q-pole	Effective mass, stiffness	He,C	>50	1000
Giant mono-pole	compressibility	He,C,...	>50	1000

Quasi elastic scattering (p,n), (³ He,t),...	IAS, r_{coul} , decay modes, GT strength	p, ³ He,	50 IAS >100 GT	10000
Stripping and transfer	Single particle properties	p,d,He	10-30	10000
Heavy ion transfer		Li,Be,C,O,...	1-20	10000
One(two) particle removal		Be,C,...	>50	1
Knock-out (p,2p) (p,pn)		p...	>50	100
Resonant scattering	Particle unbound states at p-dripline, IAS near n-dripline	p	1-20	10000

1. Deep inelastic transfer & breakup
(transparency of the optical potential).
2. Unbound exotic nuclei.
3. Giant resonances (see Chomaz's talk).

Courtesy of Livius Trache

Data on heavy neutron rich - lacking!



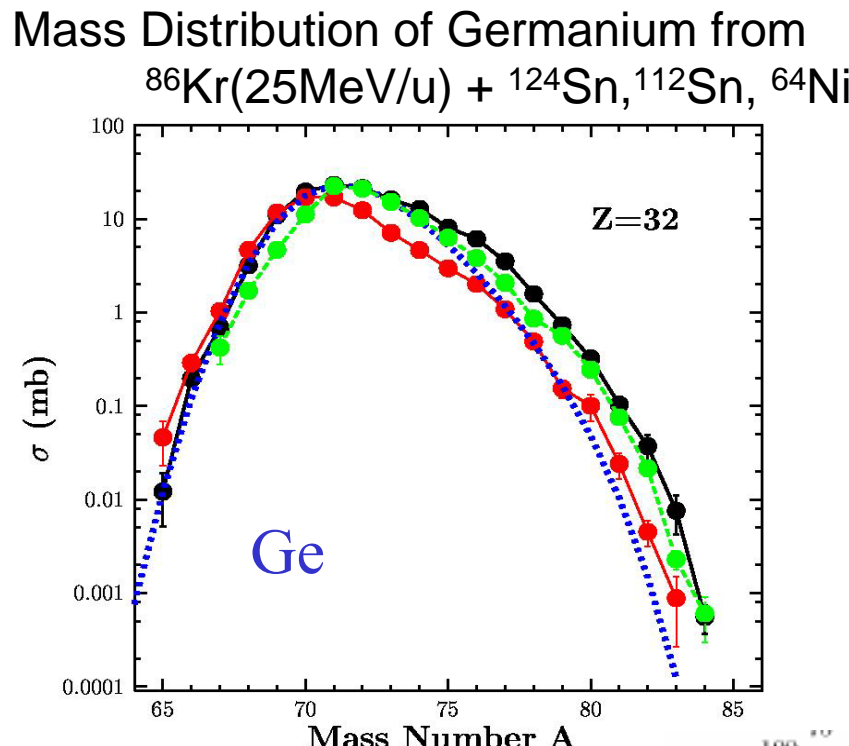
DIT mechanism can produce neutron-rich heavy residues and quasi projectiles with a diversity in N/Z

Data using targets:

- ^{124}Sn
- ^{112}Sn
- ^{64}Ni

— EPAX2

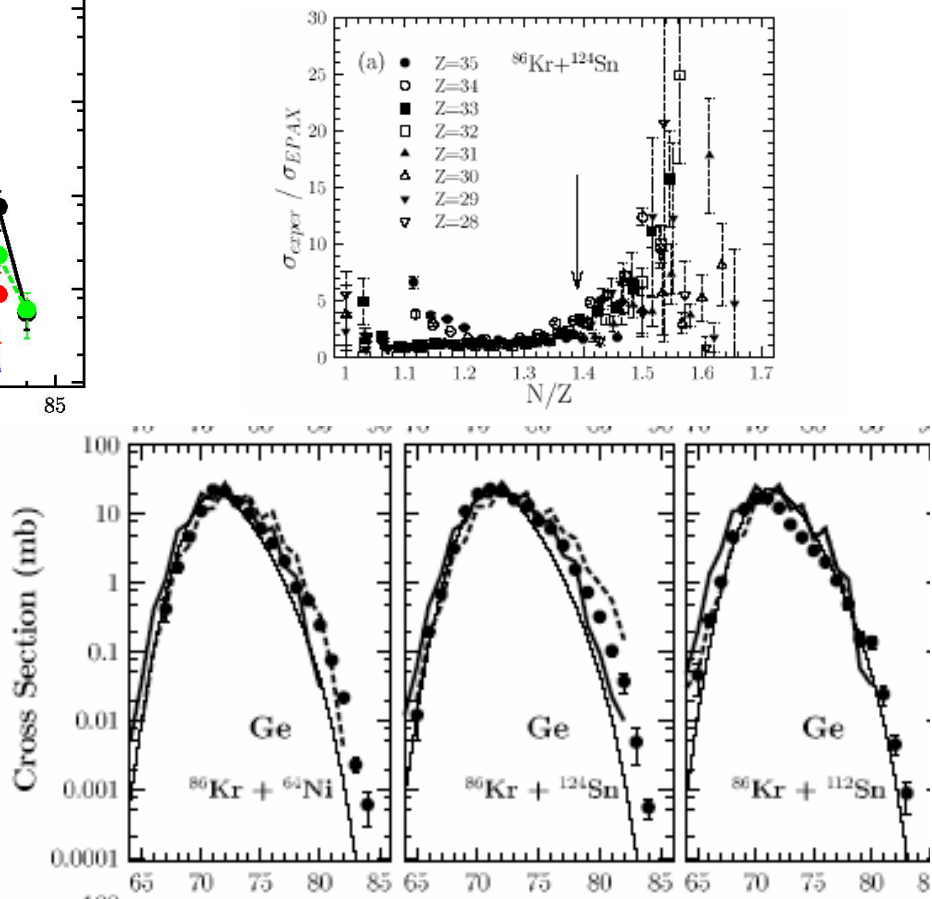
MARS data

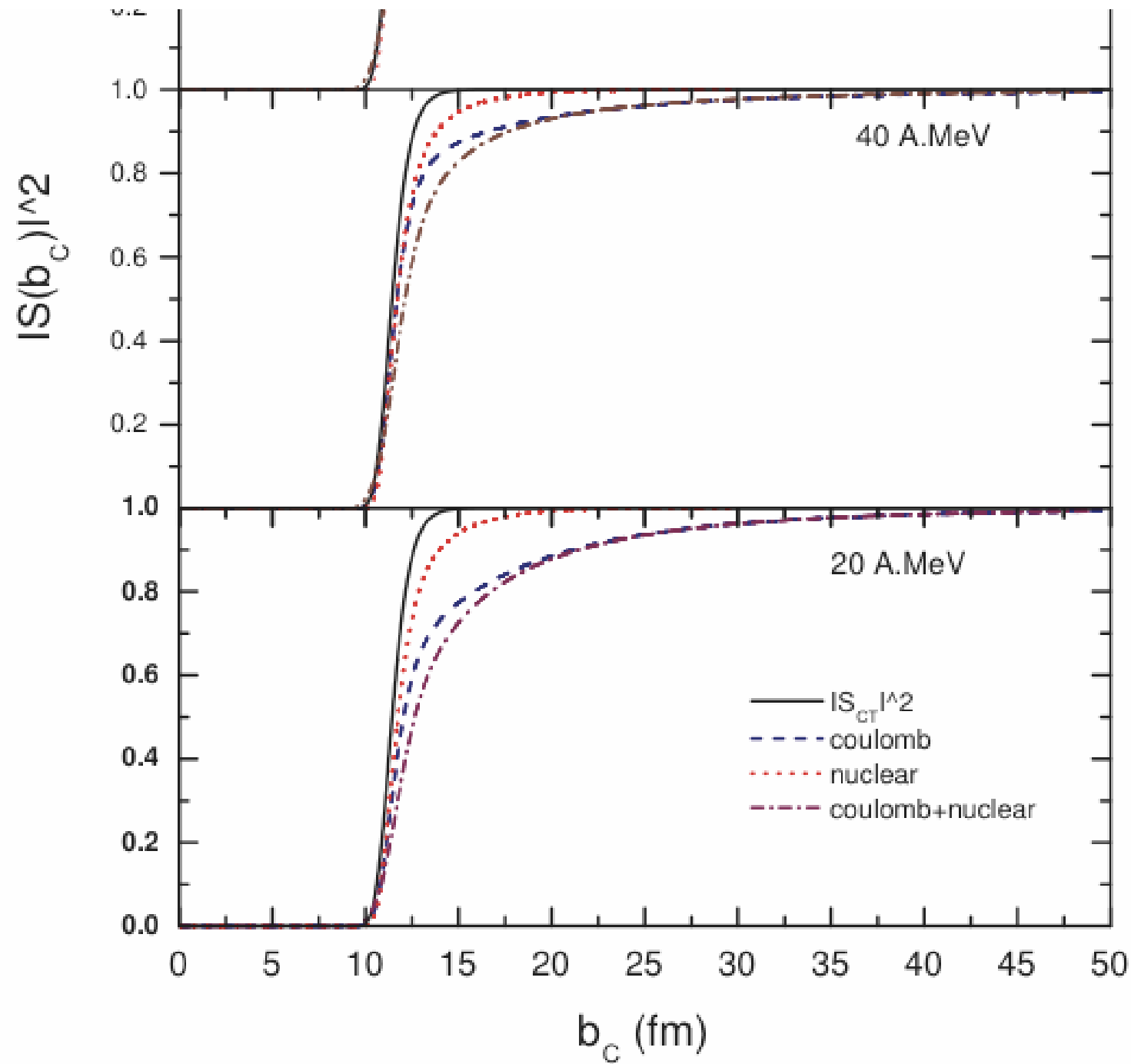
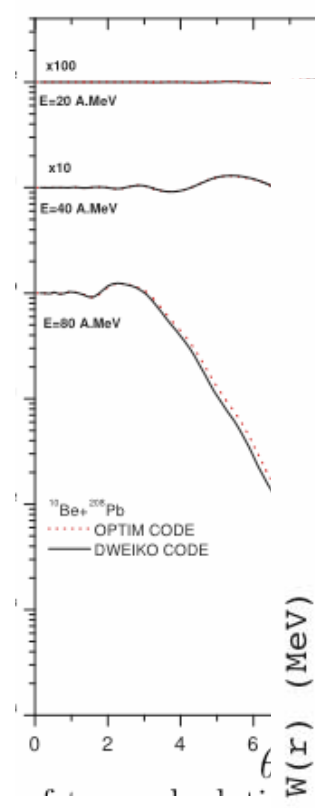


Target	N/Z	
^{124}Sn	1.48	n-rich
^{112}Sn	1.24	n-poor
^{64}Ni	1.29	n-rich

Souliotis, Phys. Rev. Lett. 91, 022701 (2003)

Calculations with DIT/GEMINI +neutron skin distributions reproduce well the ^{124}Sn and ^{64}Ni





For example, a beam of ^{92}Kr from an ISOL-type facility [or, from the proposed rare isotope accelerator facility [10,11]] can be accelerated around the Fermi energy and interact with a very neutron-rich target (e.g., ^{64}Ni , ^{124}Sn , ^{208}Pb , ^{238}U) to produce extremely neutron-rich nuclides that cannot be accessed by fission or projectile fragmentation. A quantitative prediction of rates of such nuclides will be possible after further experimental studies and improvement of the description of peripheral collisions between very neutron-rich heavy nuclei in the Fermi energy regime.

One-proton removal from loosely bound nuclei at low(er) energies

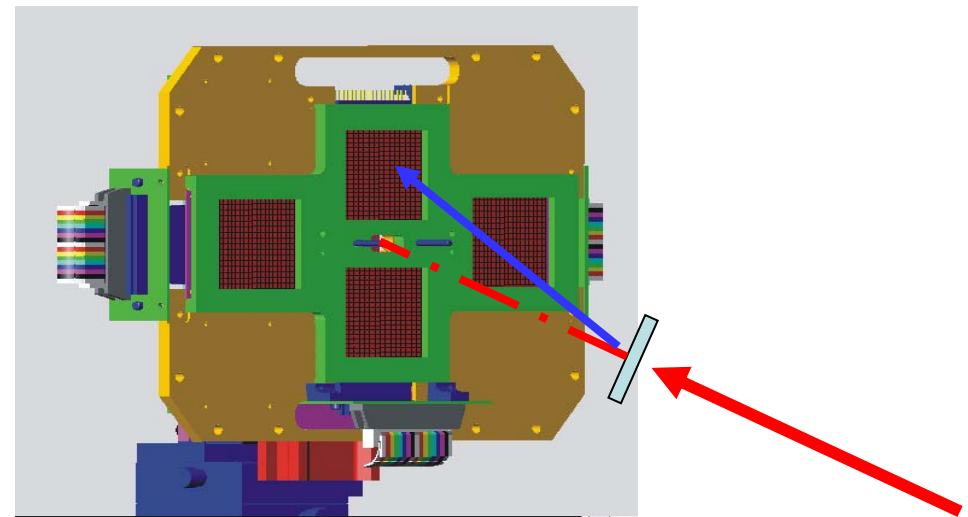
Data for projectiles with different proton separation energies:

- ^{12}N $S_p=601$ keV
- ^8B $S_p=137$ keV
- ^{13}N $S_p=1943$ keV
- ^7Be $S_p=5606$ keV
- ^{11}C $S_p=8689$ keV (not shown)

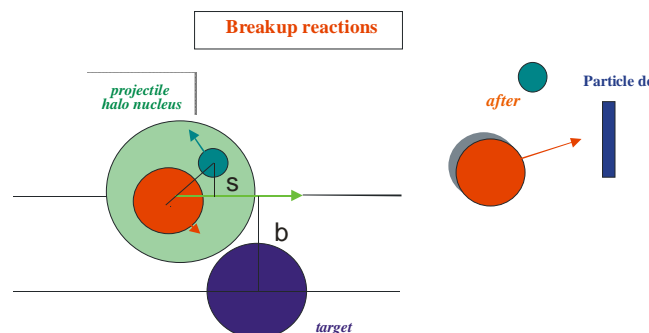
Coverage: ~ 4 – 29 deg. (lab)

Experimental data from MARS group at Texas A&M Univ.

**RNB produced with MARS:
 12 MeV/u, $\sim 10^4\text{-}10^6$ pps**



**projectile
 ~ 12 MeV/u**



All breakup data unpublished. ^7Be , ^8B , ^{11}C and ^{13}N elastic scattering and transfer data published in A. Azhari et al., PRL 82, 3960 (1999), G. Tabacaru et al., PRC 73, 025808 (2006), X. Tang et al. PRC 67, 015804 (2003) and PRC 69, 055807 (2004), respectively.

Courtesy of Livius Trache

^{12}N @ 12 MeV/u on melamine ($^{14}\text{N} + 0.5^{12}\text{C}$)

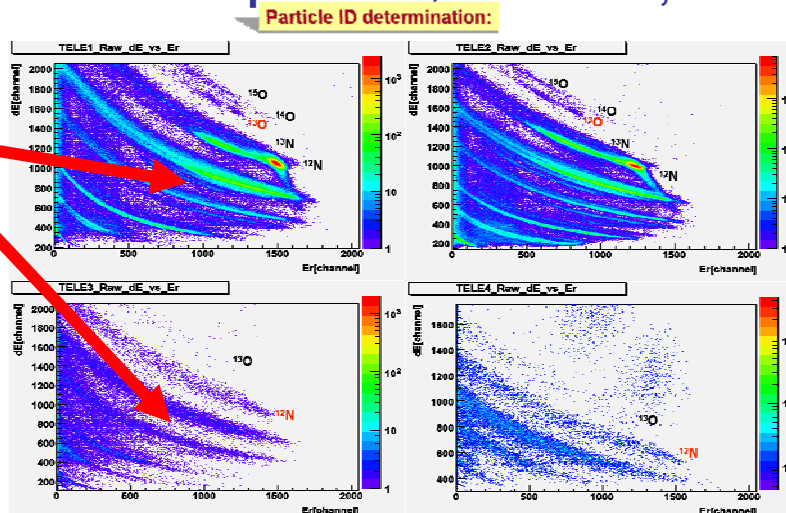
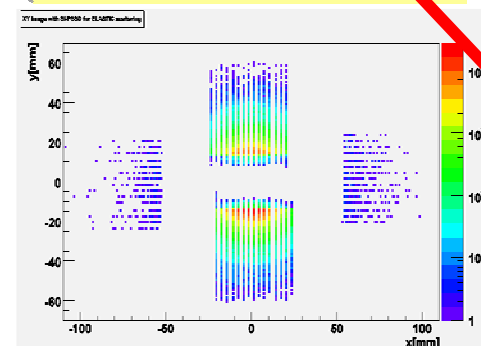
TAMU-MARS experiment, June 2006; A. Banu et al, to be published.

First Results:

$$S_p = 601.42 \pm 1.38 \text{ KeV}$$

^{11}C

Position measurement for angle determination:



$\theta = 4-15 \text{ deg.}$

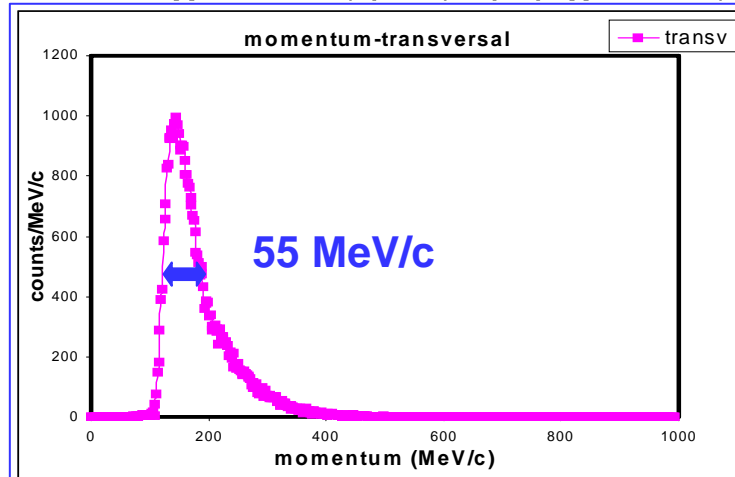
$\theta = 13-29 \text{ deg.}$

We report here preliminary results on the *asymptotic normalization coefficient* (ANC) for the system $^{13}\text{O} \rightarrow ^{12}\text{N} + \text{p}$. Our result along with information on resonant capture into excited states of ^{13}O will determine the astrophysical S factor of the $^{12}\text{N}(\text{p},\gamma)^{13}\text{O}$ reaction.
To test the scenario for stellar evolution of POPULATION III stars, hydrodynamical calculations including the full nuclear reaction network with the latest rates are necessary !

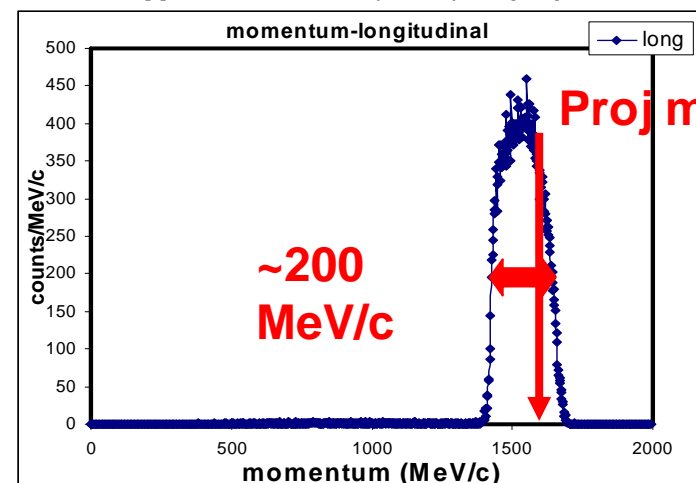
References:

- [1] G.M. Fuller et al., Ap.J. 367, 675 (1996).
- [2] M. Wiescher et al., Ap.J. 349, 352 (1990).
- [3] A.M. Mukhamedzhanov et al., JETP Lett. 51, 282 (1990).
- [4] L. Trache et al., PRC 61, 024612 (2000).
- [5] J.P. Jeukenne et al., PRC 16, 80 (1977).
- [6] M. Rhoades-Brown et al., PRC 21, 2417 (1980)

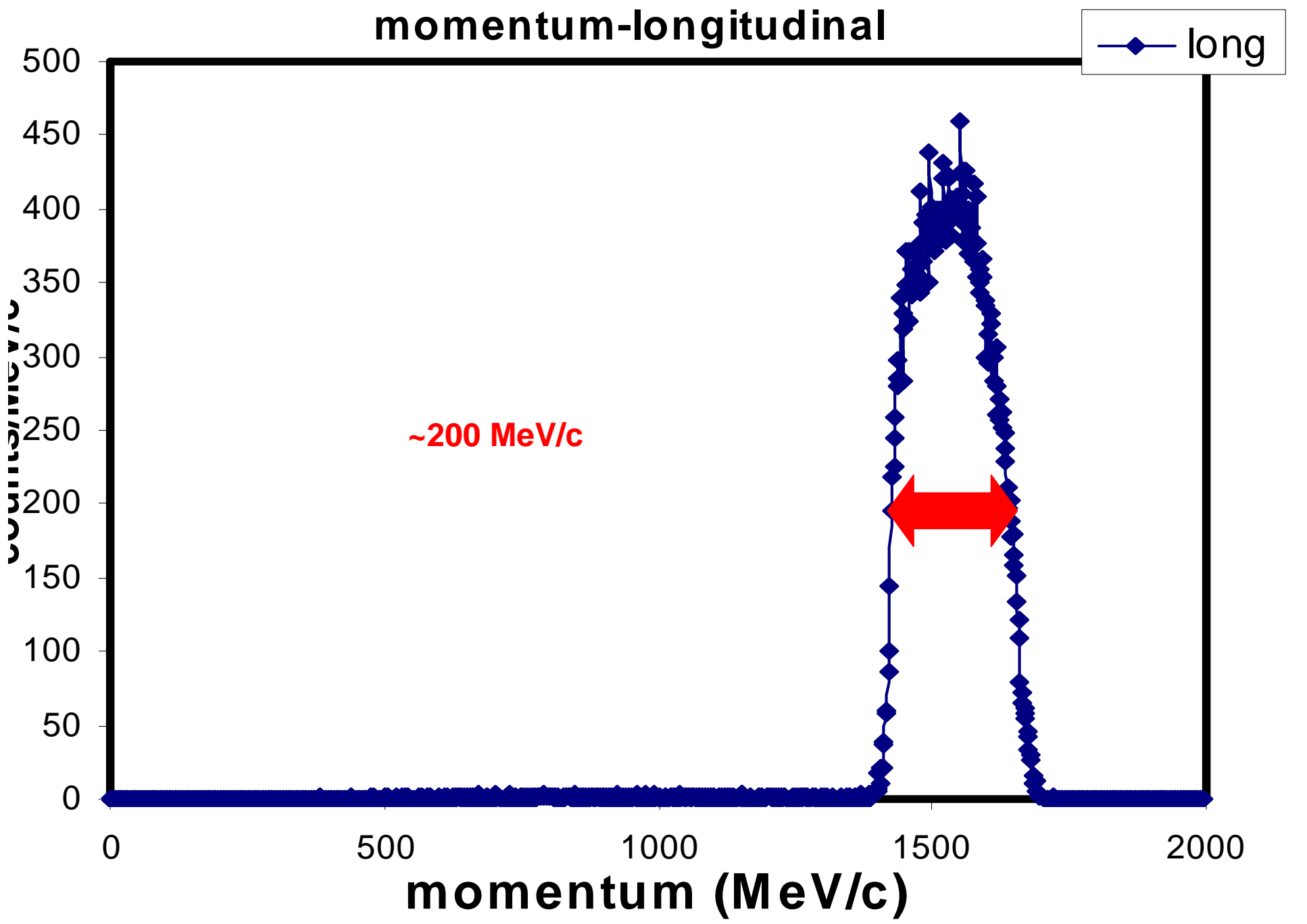
^{11}C momentum distributions



55 MeV/c



~ 200 MeV/c
Proj mom



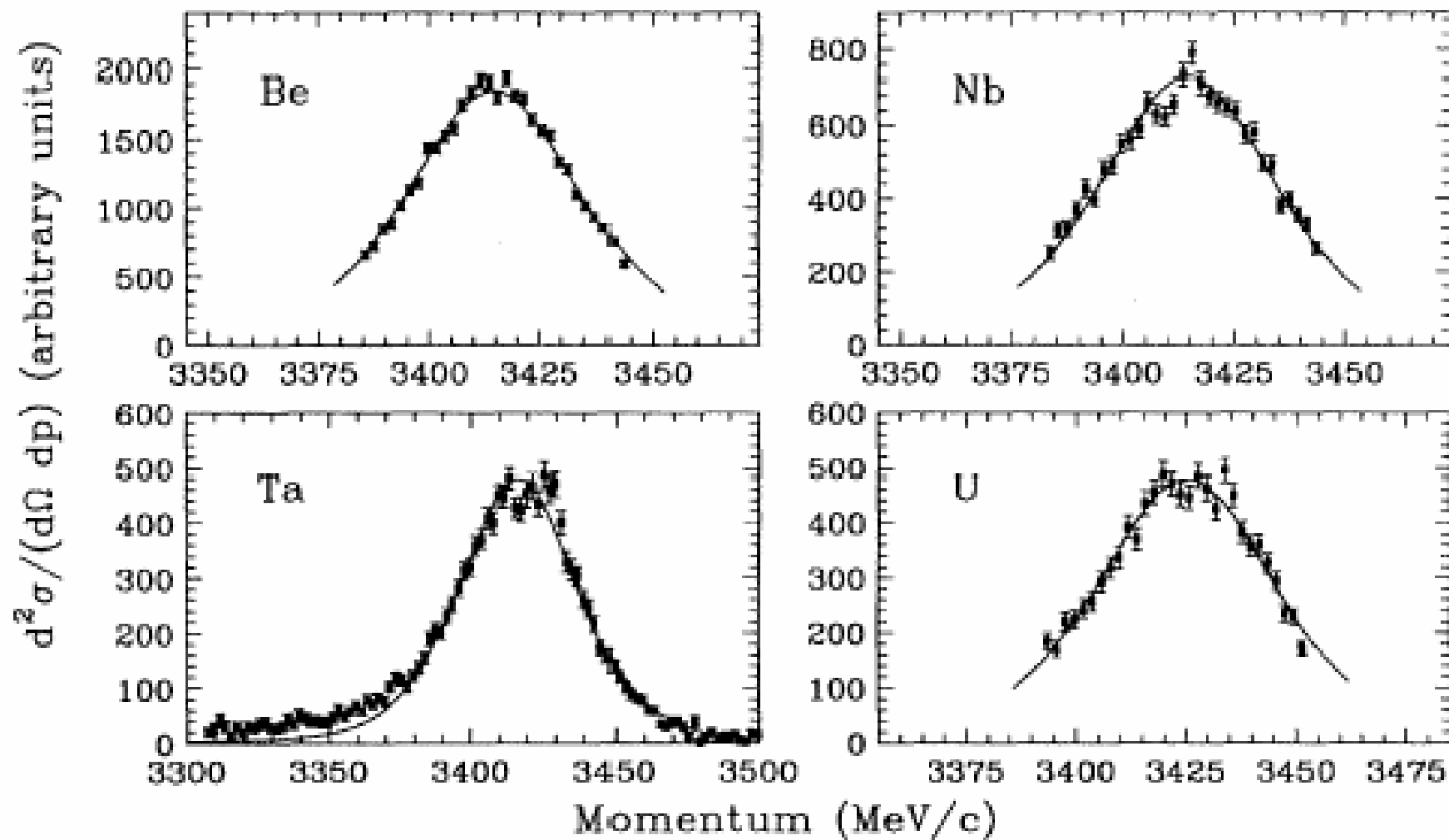


FIG. 1. The $p_{||}$ distributions of ^{10}Be fragments from the breakup of ^{11}Be on various targets. The data are corrected for efficiency of transmission to the focal plane. Additional

${}^8\text{B}$:

$$S_p = 137.46 \pm 1.00 \text{ KeV}$$

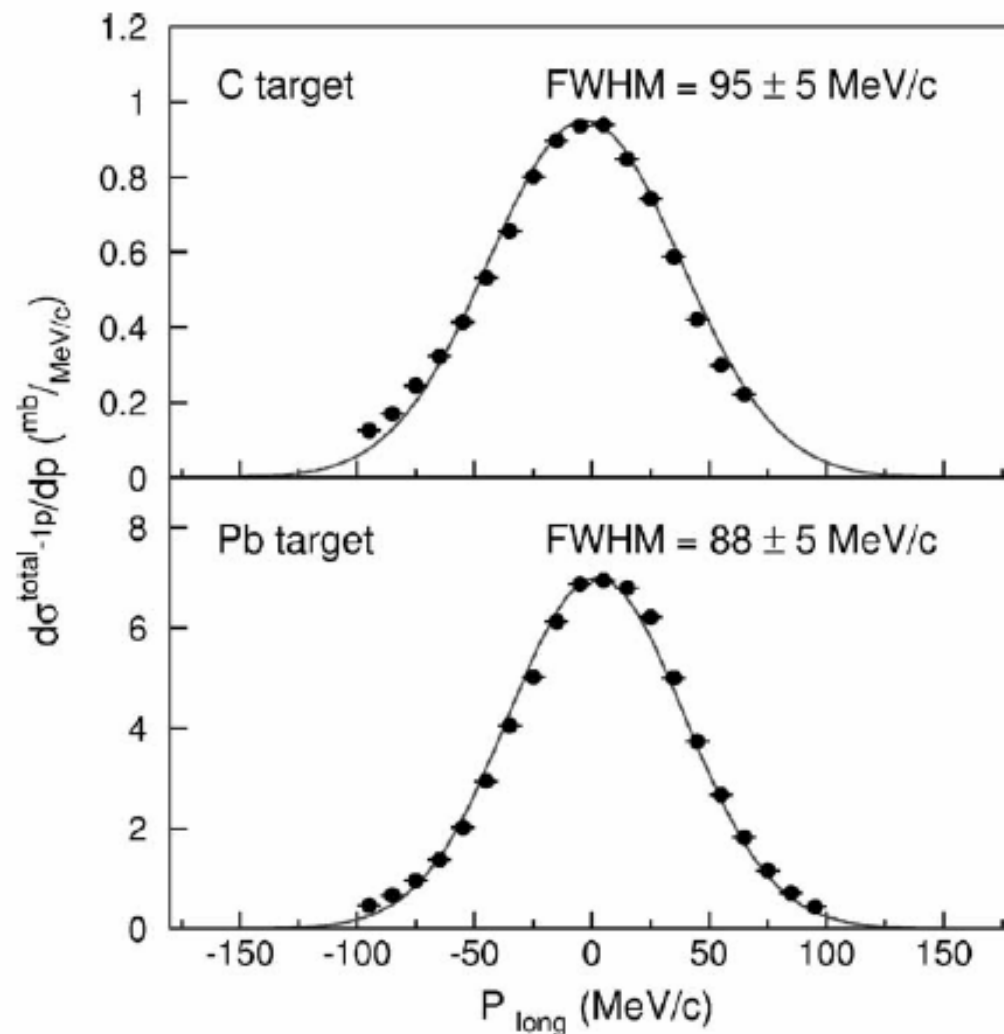
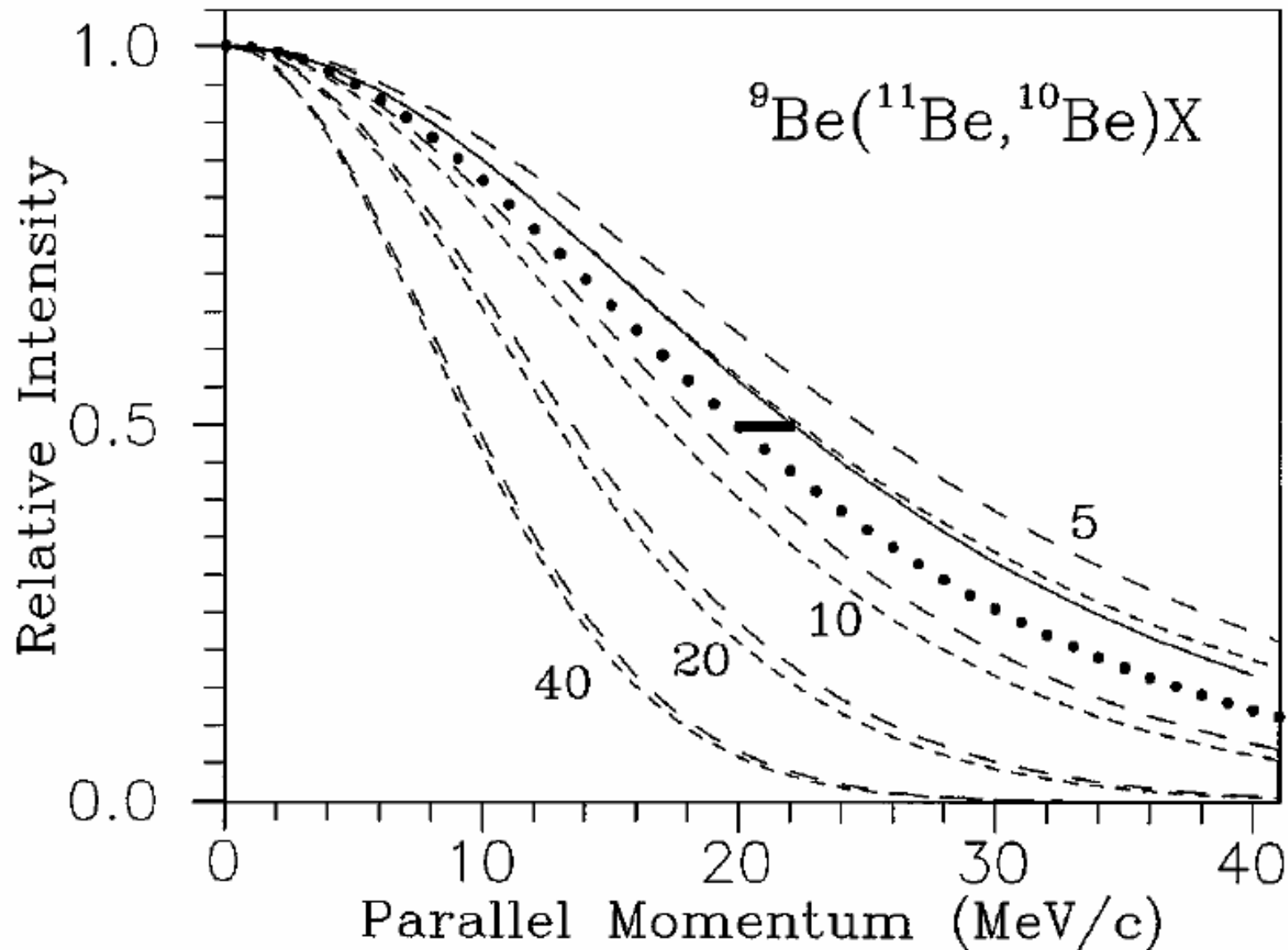
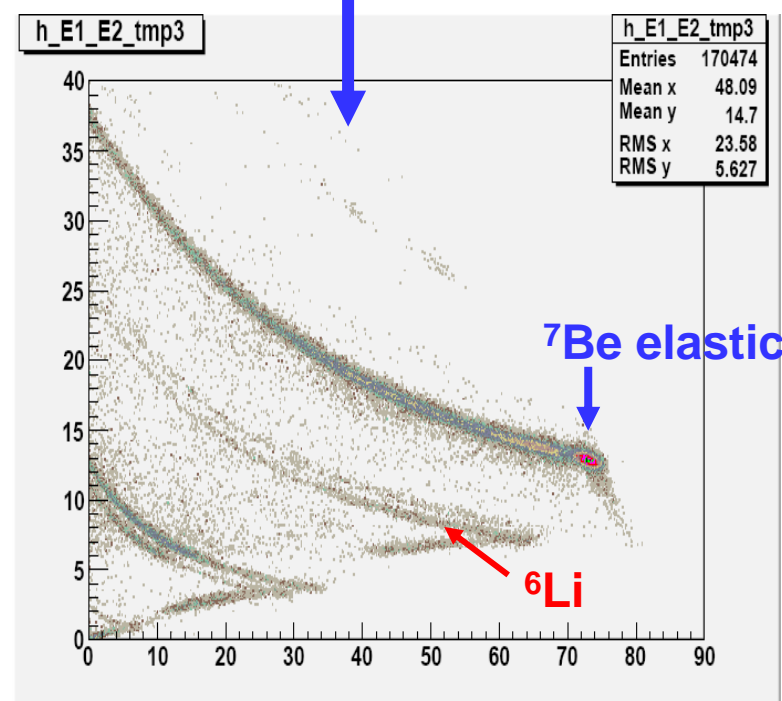
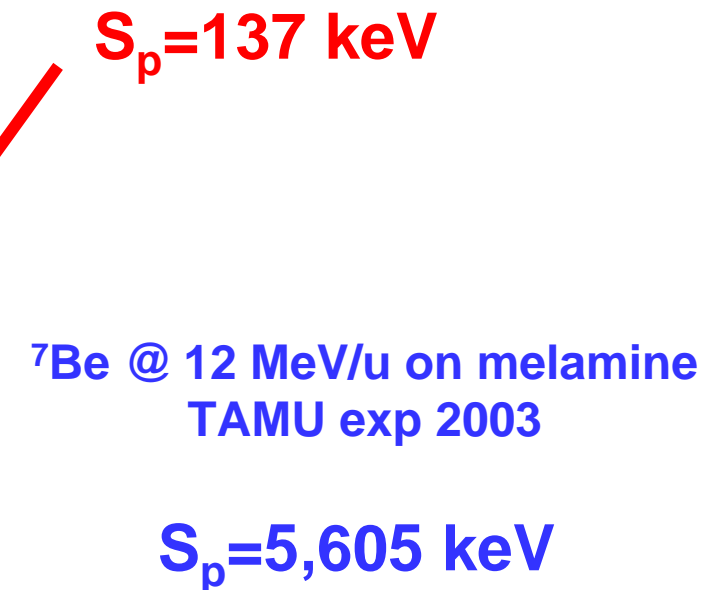
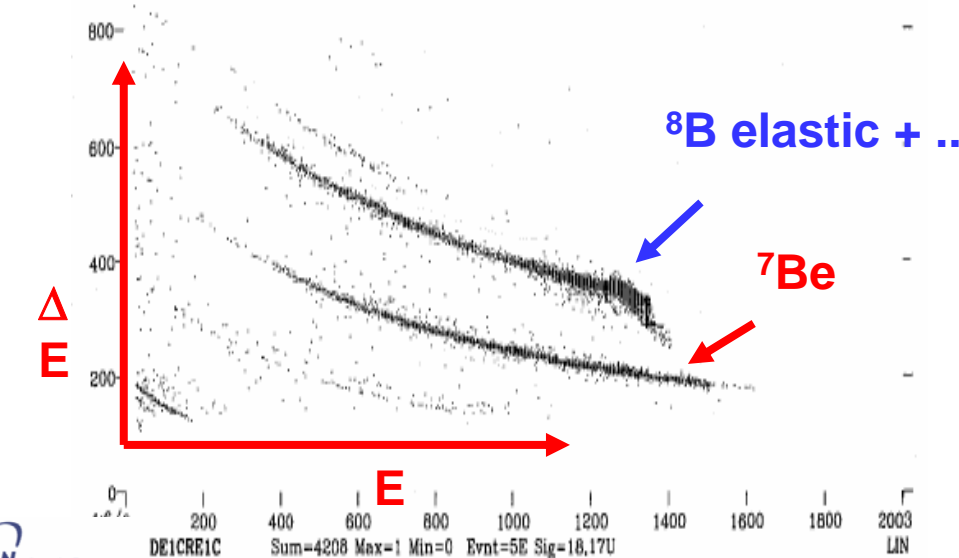
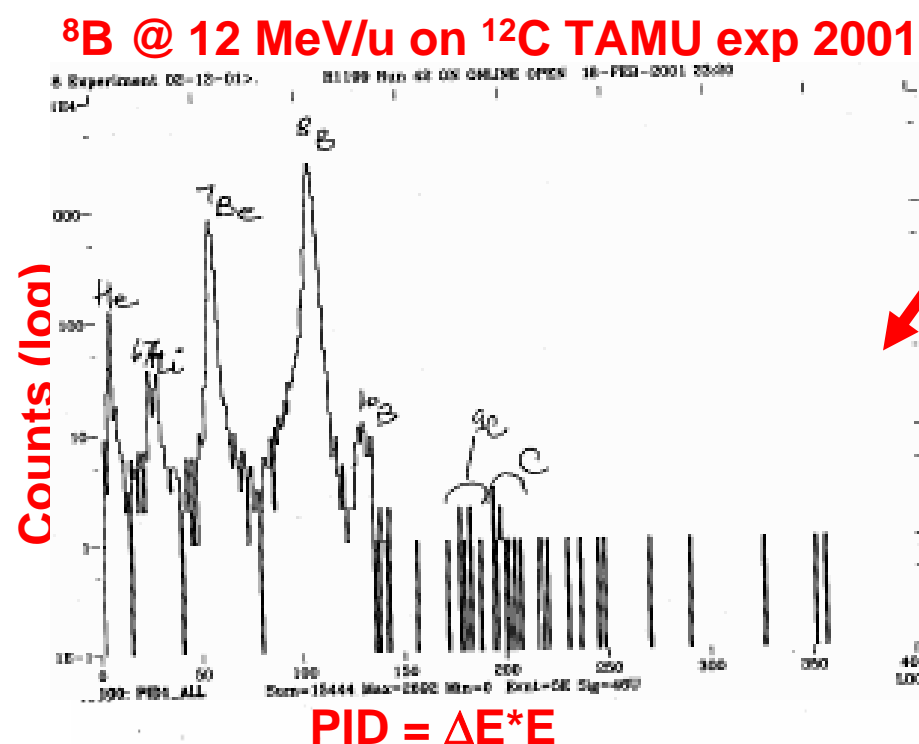


Fig. 4. ${}^7\text{Be}$ longitudinal momentum distributions after breakup of ${}^8\text{B}$ for C (top) and Pb (bottom) targets normalized to the corresponding one-proton removal cross sections (σ_{-1p}). The solid lines correspond to Gaussian fits used to evaluate the FWHM.

PG Hansen, PRL77(1996)1016





^{13}N @ 12 MeV/u on melamine and C

PHYSICAL REVIEW C 69, 055807 (2004)

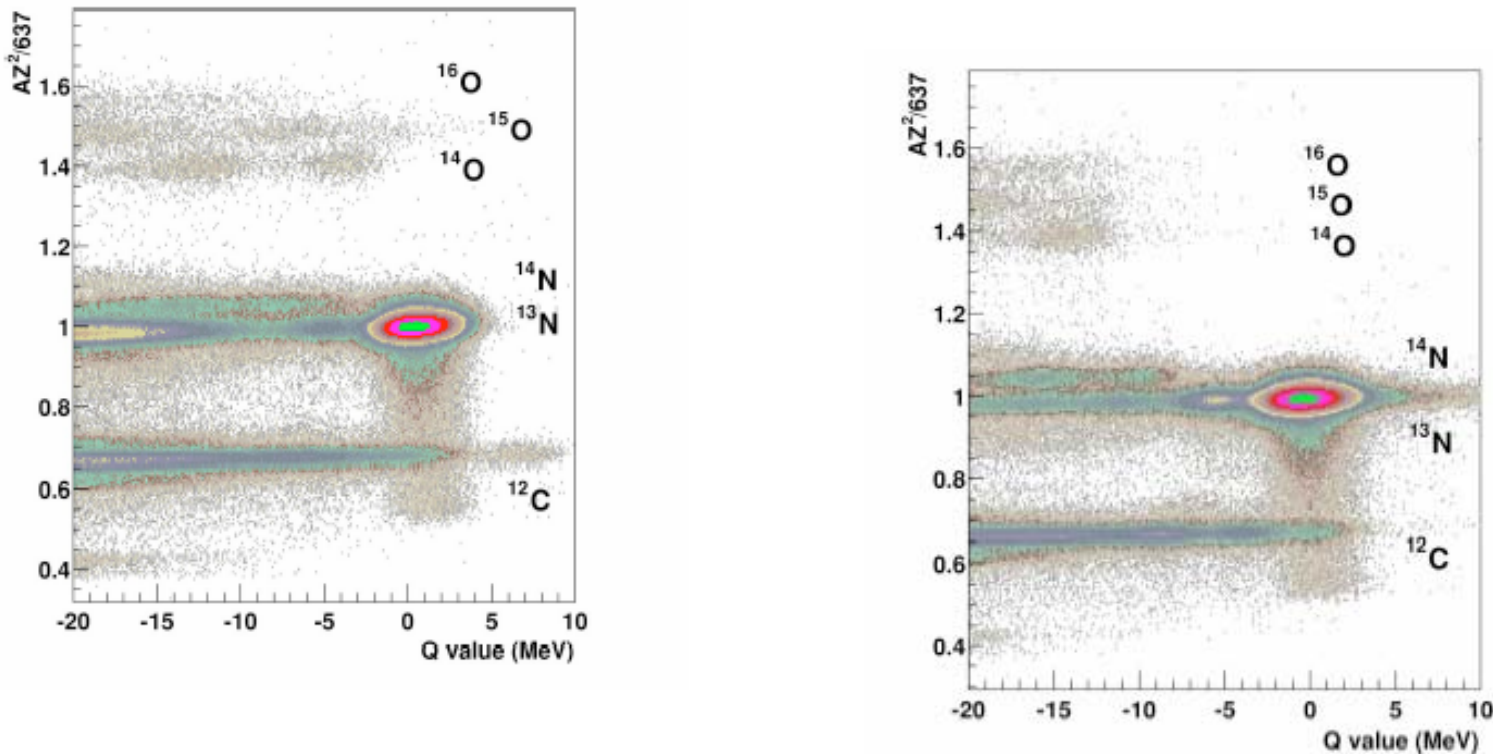
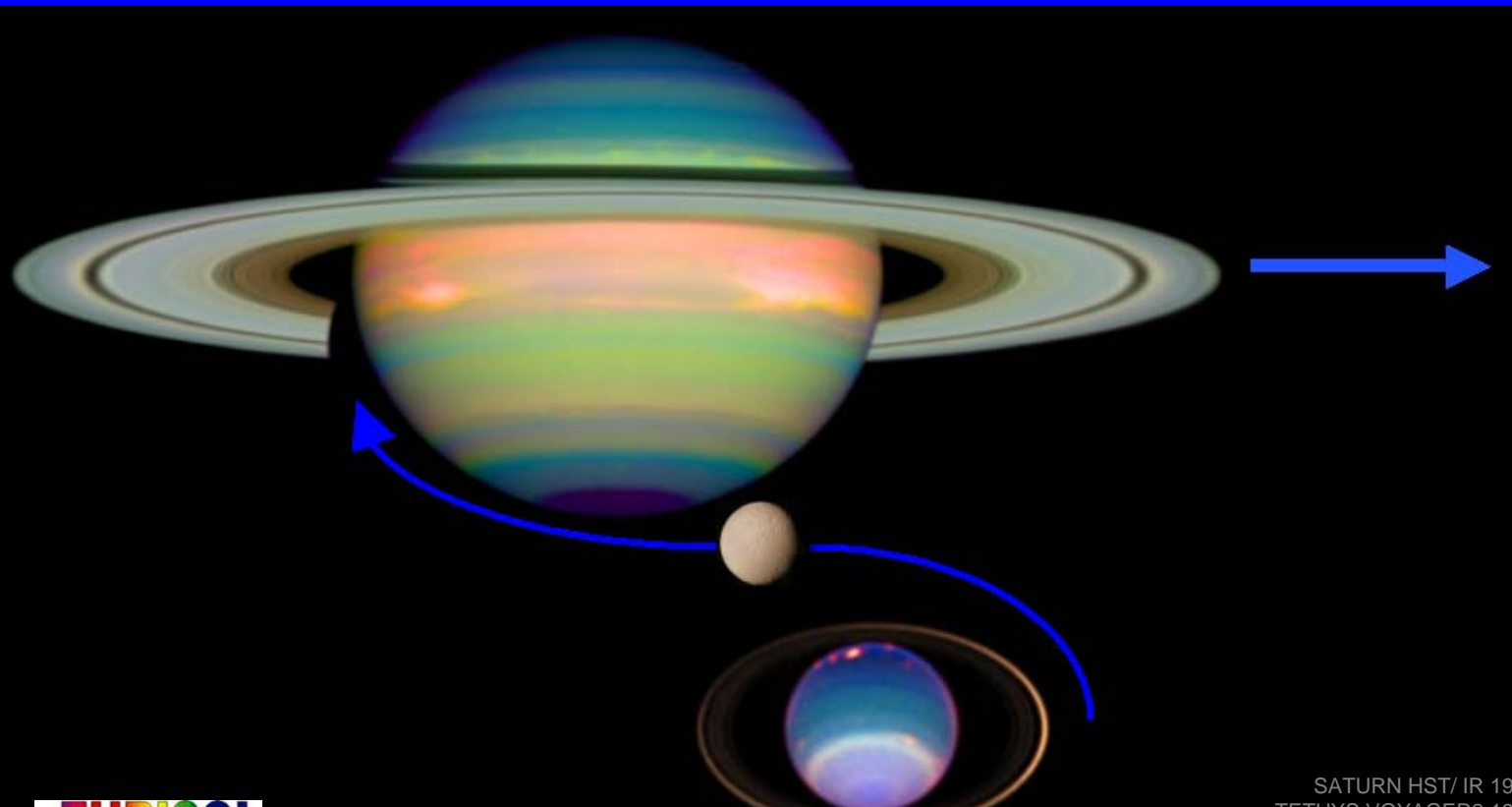


FIG. 3. (Color online) The particle identification vs Q -value distribution from the melamine (top panel) and C (bottom panel) targets. The ^{13}N group with Q value of 0 MeV is the elastic scattering off the C and N in the melamine target. There was a small Ta contaminant in the C foil that appears as a tail to positive Q value. In the spectrum from the melamine target, the broad peak with a Q value of about -20 MeV is due to elastic scattering off H and the least negative Q value peak in ^{14}O is from $^{14}\text{N}(^{13}\text{N}, ^{14}\text{O})^{13}\text{C}_{\text{g.s.}}$.

Charged Particles : How do we go about detecting them?



EURISOL

28-29 NOV 2005

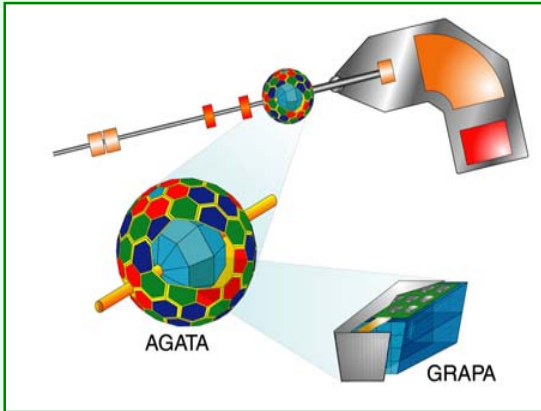
SATURN HST/ IR 1998
TETHYS VOYAGER2 1981
URANUS HST/ IR 1986

Wilton Catford

University of Surrey, Guildford, UK

Deep inelastic

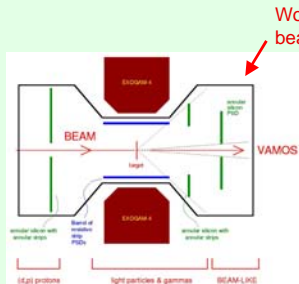
EURISOL Project - GRAPA



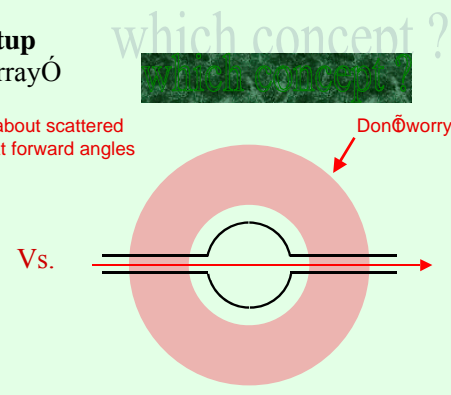
EURISOL Reactions Subarou 2001

Emanuel POLLACCO
CEA SACLAY

Transfer/Inelastic/Elastic setup N^{π} Reaction Spectroscopy Array



Intense beams $> 10^8$ pps

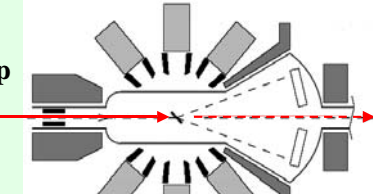


Weak beams $< 10^5$ pps
or
highly segmented gamma array

EURISOL: Experiments that need to detect charged particles

This leaves us with three basic concepts:

□ Coulex/Deep Inelastic type of setup



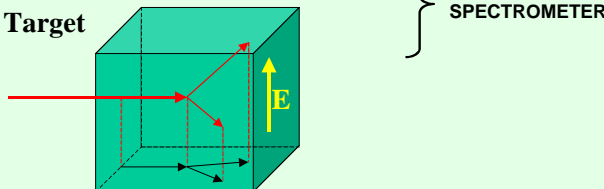
□ Transfer/Inelastic/Elastic setup

also: *fusion-evaporation*

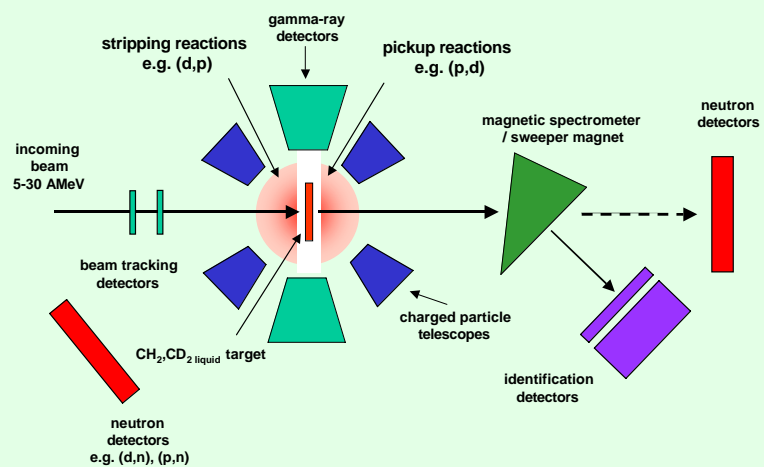
N^{π} Reaction Spectroscopy Array

È of which, more in a moment

□ TPC or Active Target



Fixed Target Measurements of Direct Reactions



SLIDE BORROWED FROM R.C. LEMMON

Unbound exotic nuclei.

Excited states of ${}^7\text{He}$, ${}^5\text{H}$

${}^{26,28}\text{O}$: limits of stability
(N=20, *island of inversion*)

Patricia Russel-Chomaz

Collaboration: GANIL, RIKEN, JINR Dubna

Spectroscopy of unbound H and He isotopes : ^5H , ^7He

^5H : experimental situation not clear

$t(t,p)^5\text{H}$ reaction : structure observed at 1.8 MeV above $t+n+n$ threshold

P.G. Young et al. Phys. Rev. 173 (1968) 949

$^9\text{Be}(\pi^-, p t)^5\text{H}$: structure at " 7 MeV, $^9\text{Be}(\pi^-, dd)^5\text{H}$: no structure

M.G. Gornov et al., Nucl. Phys. A531 (1991) 613

$^7\text{Li}(^6\text{Li}, ^8\text{B})^5\text{H}$: structure at " 5 MeV

D.V. Aleksandrov et al., Proc. ENAM 95

Present work ${}^6\text{He}(p, pp){}^5\text{H}$

Proton pick-up in ${}^6\text{He}$ --> selective population of ${}^5\text{H}$ ground state

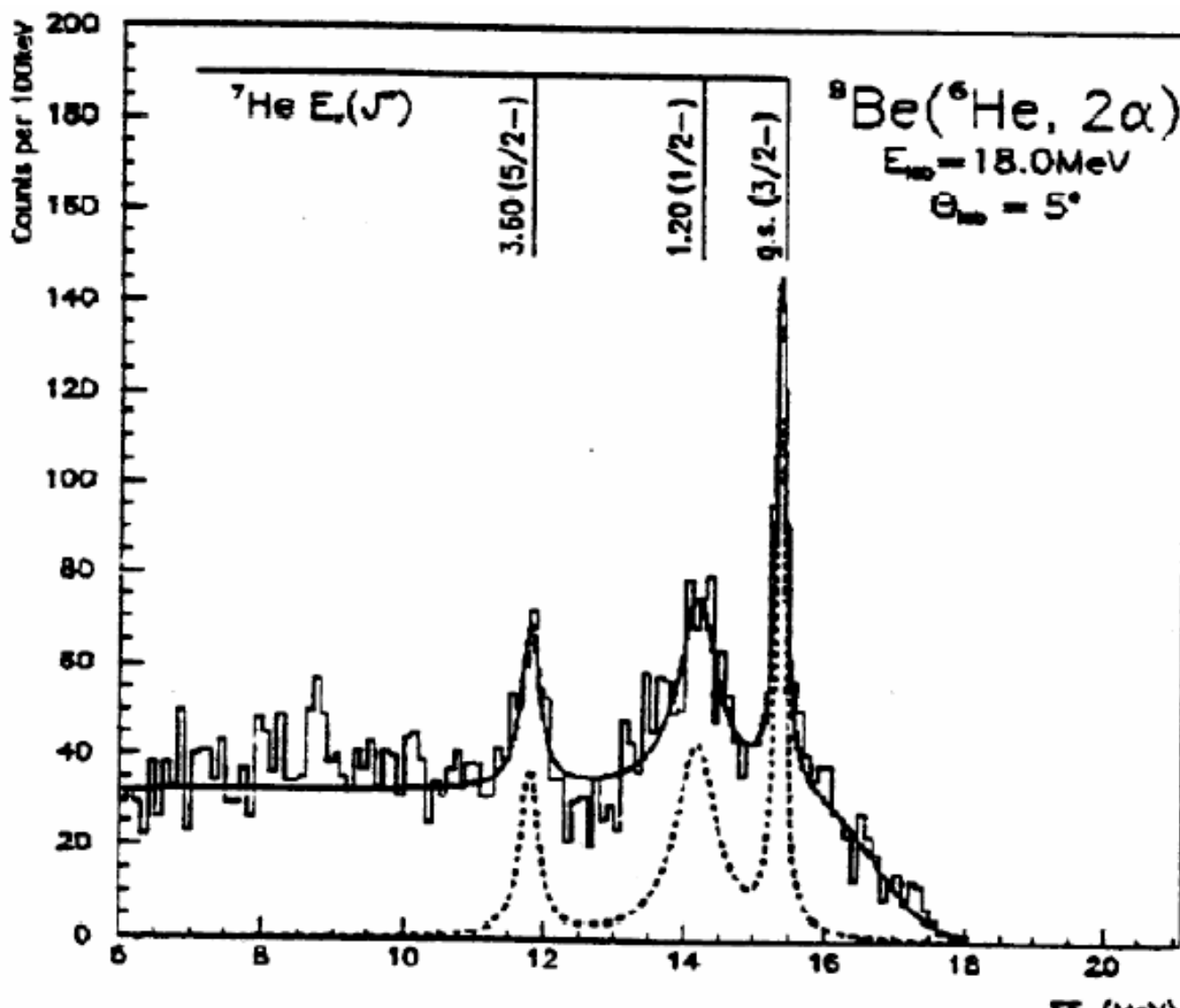
${}^7\text{He}$: ground state well known, ($E^* = 440$ keV, $\Gamma = 160$ keV), excited states?

${}^8\text{He}(p, d){}^7\text{He}$, $E^* = 2.9(3)$ MeV, $\Gamma = 2.2(3)$ MeV, A.A. Korsheninnikov et al., PRL 82(99) 3581

${}^9\text{Be}({}^{15}\text{N}, {}^{17}\text{F}){}^7\text{He}$, $E^* = 2.95(10)$ MeV, $\Gamma = 1.9(3)$ MeV, H.G. Bohlen et al., PRC 64(01) 024312

${}^8\text{He}$ dissociation, $E^* = 0.8(2)$ MeV, $\Gamma = 1.2(2)$ MeV, K. Markenroth et al., NPA 679(01) 462

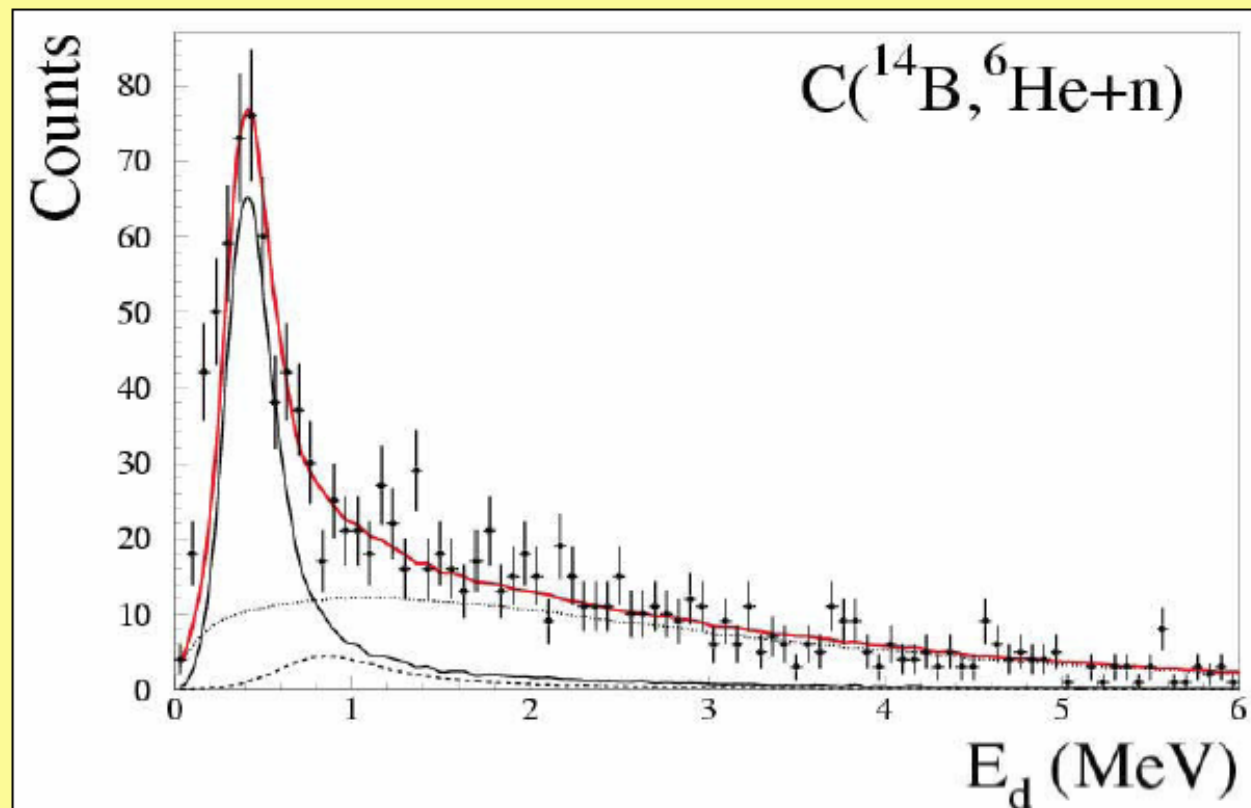
Present work ${}^6\text{He}(d, p){}^7\text{He}$



A.N. Ostrowski et al., Annual Report
 Louvain-la-Neuve 2000

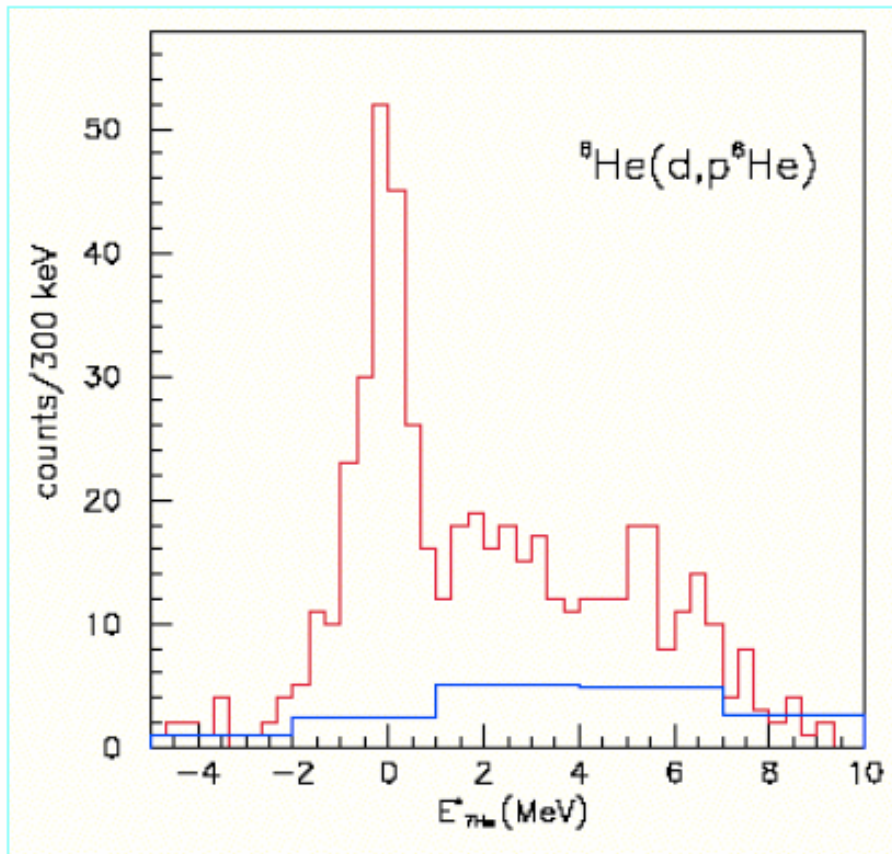
Benchmark System - ${}^7\text{He}$

Ground state ($3/2^-$) : $E_r=0.44$, $\Gamma_0=0.16$ MeV



[spin-orbit partner $E_r (1/2^-) = ??? \dots$ a "4:00pm question"]

$^6\text{He}(\text{d},\text{p})^7\text{He}$



- Ground state $E^*=0.44$ MeV above $^6\text{He}+\text{n}$ threshold, $3/2^-$, clearly observed
- No clear indication for $1/2^-$ et $5/2^+$ excited states

M.S. Golovkov et al., Proc. « Nuclear Structure and Related Topics »
Dubna June 2000.

Trends in experimental studies of exotic nuclei

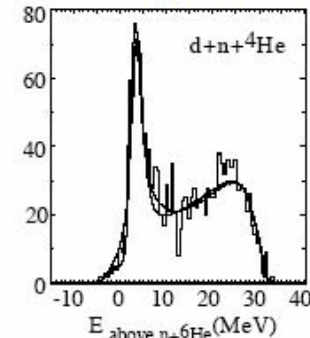
A. Korsheninnikov
RIKEN, Wako, Japan

INPC2003

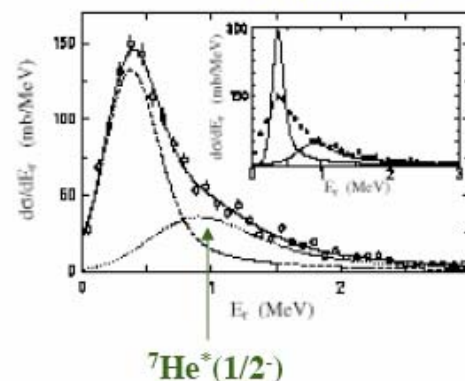
on leave from the Kurchatov Institute, Moscow

Spectroscopy of ${}^7\text{He}$

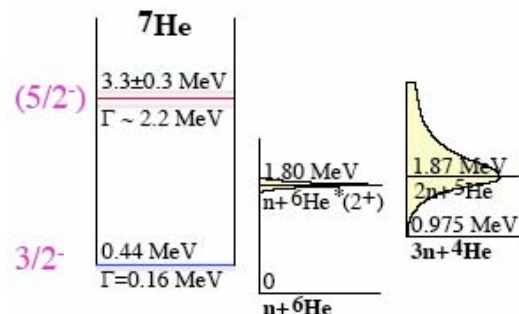
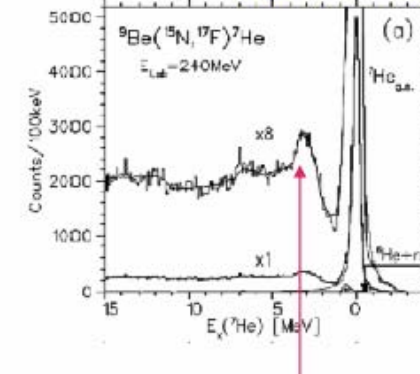
A.K. et al., Phys. Rev. Lett. **82**
(1999) 3581 $\text{p}({}^8\text{He}, \text{d}){}^7\text{He}$



M. Meister et al., Phys. Rev. Lett. **88**
(2002) 102501 $\text{C}({}^8\text{He}, \text{n}{}^6\text{He})$



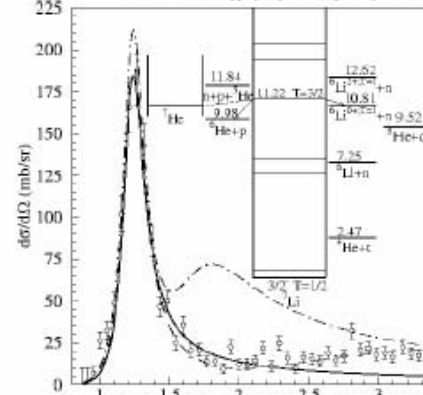
H.G. Bohlen et al., Phys. Rev. **C64**
(2001) 024312 ${}^9\text{Be}({}^{15}\text{N}, {}^{17}\text{F}){}^7\text{He}$



Theory predicts ${}^7\text{H}^*(5/2^-)$:
J. Wurzer and H.M. Hofmann, Phys. Rev. **C55** (1997) 688;
S.C. Pieper et al., Phys. Rev. **C64** (2001) 014001

G.V. Rogachev et al., Phys. Rev. Lett. **92** (2004) 232502

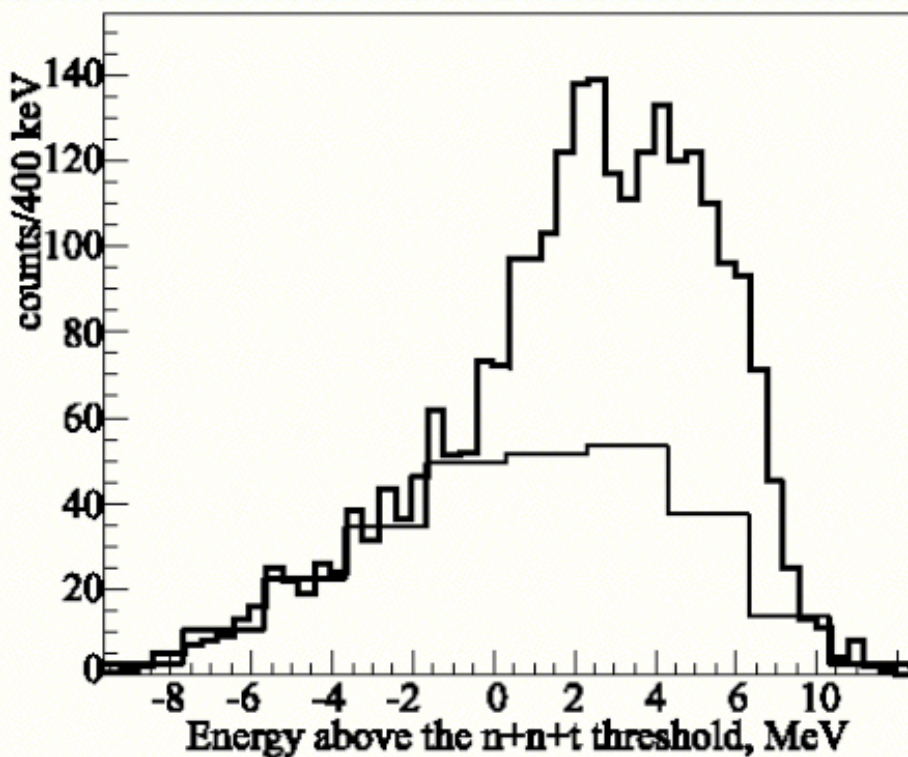
Notre Dame ${}^6\text{He}(\text{p}, \text{n}){}^6\text{Li}(0^+, \text{T}=1)$



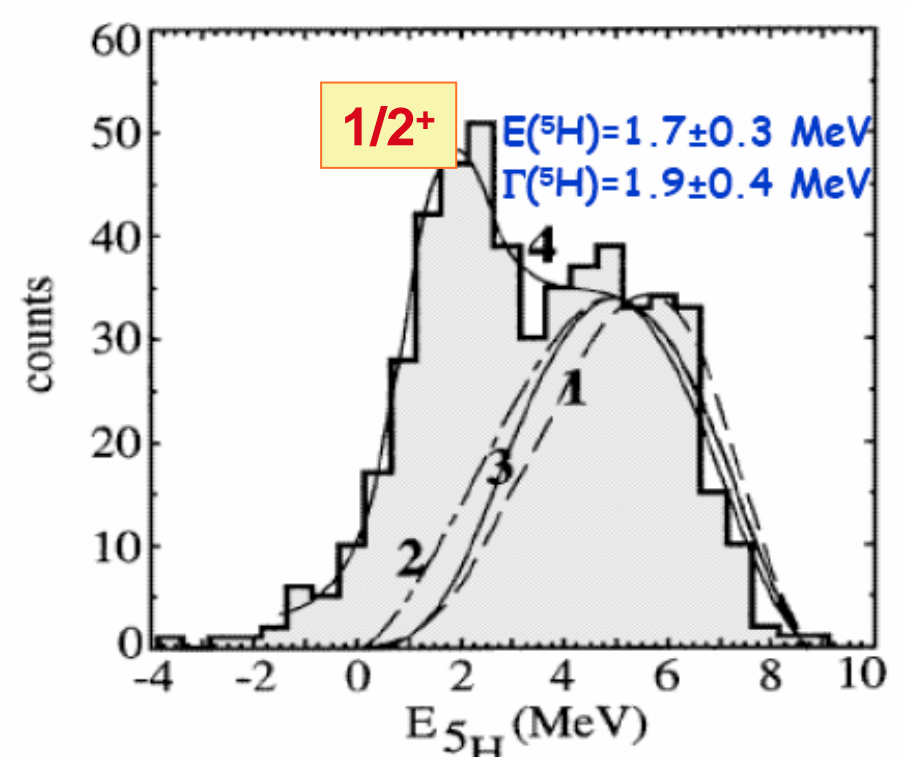
$^6\text{He}(\text{p},2\text{p})^5\text{H}$

- Missing mass method, with unbound recoil (2p)

Coincidence p+p



Coincidence p+p+t

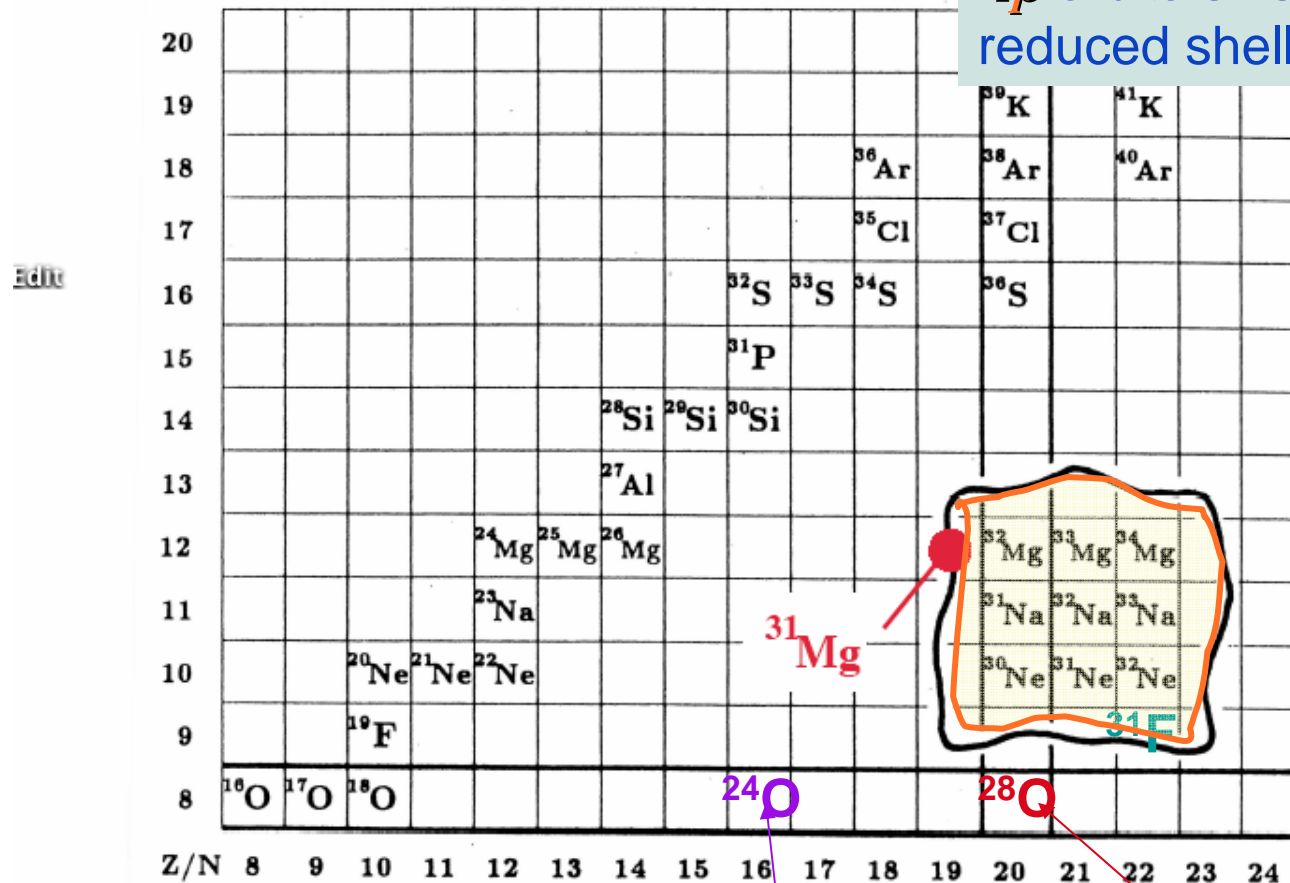


A.A. Korsheninnikov et al. Phys. Rev. Lett. 87 (2001) 092501

Limits of stability $^{26,28}\text{O}$: 2p knockout from $^{28,30}\text{Ne}$

(N=20, *island of inversion*)

deformed ground state intruder
 fp orbitals vs. sd spherical,
reduced shell gaps



N=16 new magic

last particle stable,
doubly magic?(N=16)

only weakly unbound

Figure 1: “Island of inversion”, the tentative borders are taken from Ref. [4] (apart from the “island” only stable nuclei are shown). The red dot marks ^{31}Mg .

Status of art

Study of ^{10}Li via the $^{9}\text{Li}(\text{H},\text{p})$ reaction at REX-ISOLDE

H.B. Jeppesen ^{a,b,*}, A.M. Moro ^c, U.C. Bergmann ^b, M.J.G. Borge ^d, J. Cederkäll ^b, L.M. Fraile ^b, H.O.U. Fynbo ^a, J. Gómez-Camacho ^c, H.T. Johansson ^e, B. Jonson ^e, M. Meister ^e, T. Nilsson ^{e,f}, G. Nyman ^e, M. Pantea ^f, K. Riisager ^{a,b}, A. Richter ^f, G. Schriener ^f, T. Sieber ^g, O. Tengblad ^d, E. Tornqvist ^e, M. Tytgat ^d, T. Winther ^b

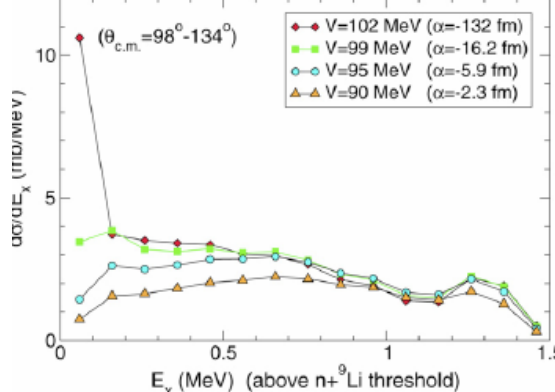


Fig. 2. (Color online.) Calculated excitation energy spectrum for $\text{p}(\text{H},\text{p})^{10}\text{Li}$ leading to $\ell = 0$ states in the $^{10}\text{Li}(=^{9}\text{Li} + \text{n})$ system. The x -axis corresponds to the excitation energy in the ^{10}Li system. The $\text{i} + \text{n}$ potential is a Gaussian with potential radius $a = 2$ fm, and depths indicated by the labels in the insert.

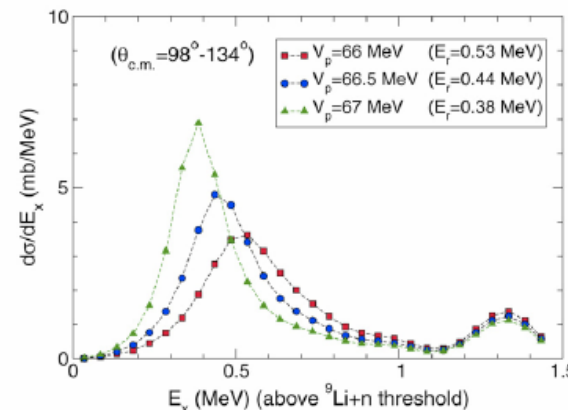
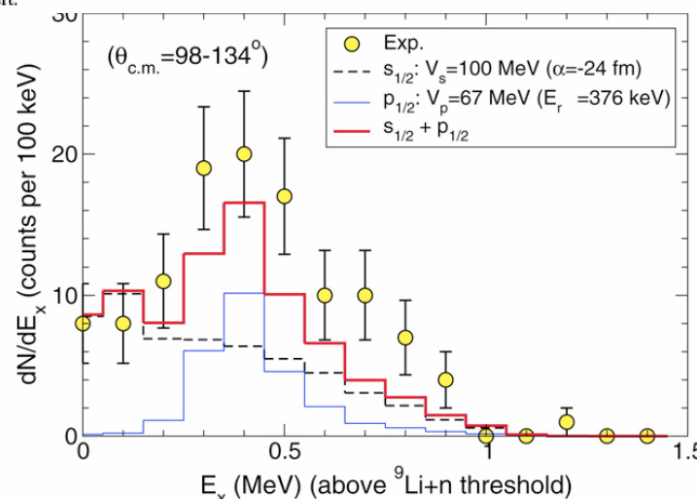


Fig. 3. (Color online.) Calculated excitation energy spectrum for the reaction $^{9}\text{Li}(\text{H},\text{p})^{10}\text{Li}$ leading to $\ell = 1$ ($p_{1/2}$) states in the $^{10}\text{Li}(=^{9}\text{Li} + \text{n})$ system. The abscissa corresponds to the excitation energy in the ^{10}Li system above the neutron- ^{9}Li threshold.



Unbound exotic nuclei studied by transfer to the continuum reactions

G. Blanchon ^a, A. Bonaccorso ^{a,*}, N. Vinh Mau ^b

G. Blanchon et al. / Nuclear Physics A 739 (2004) 259–273

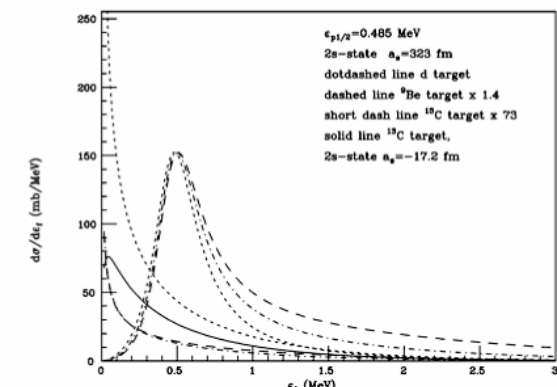
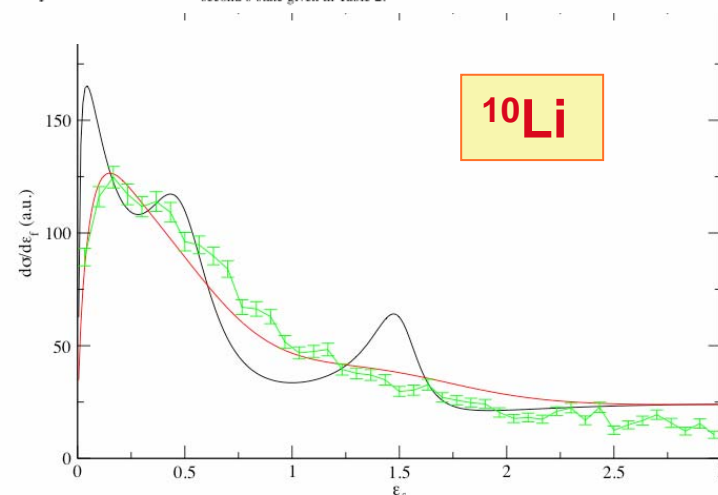


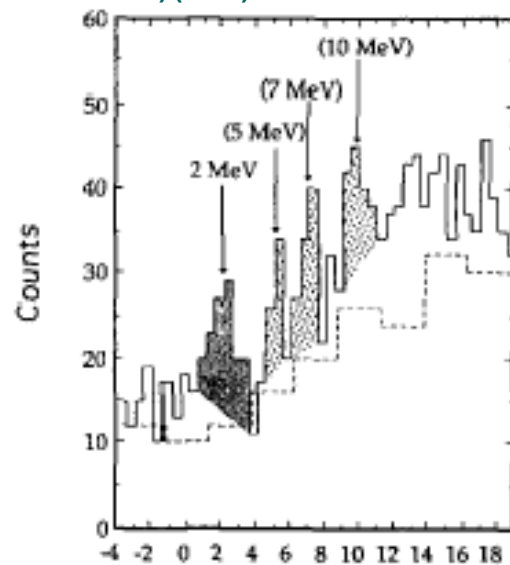
Fig. 2. Neutron- ^{9}Li relative energy spectra for transfer to the s and p continuum states in ^{10}Li given in Table 2. Dotted lines are absolute cross sections for transfer from a deuteron target, dashed lines from a ^{9}Be target, and short dashed line from a ^{13}C target. The Be and C cross section have been renormalized to the deuteron cross sections by the factors indicated on the figure. The solid line is the transfer cross section from the C target to the second s-state given in Table 2.



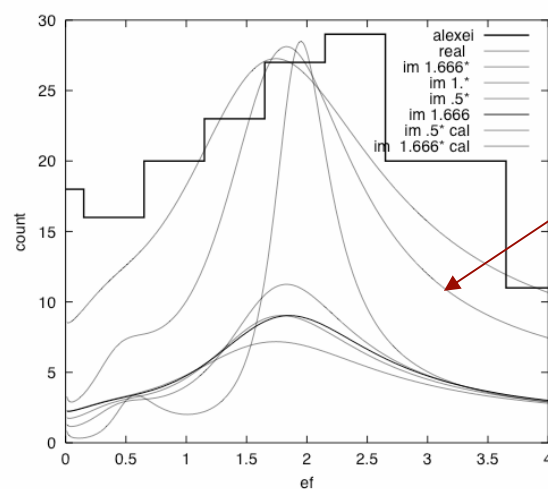
^{13}Be : an example of creation by the reaction mechanism

- transfer to the continuum: ^{12}Be (d,p) RIKEN

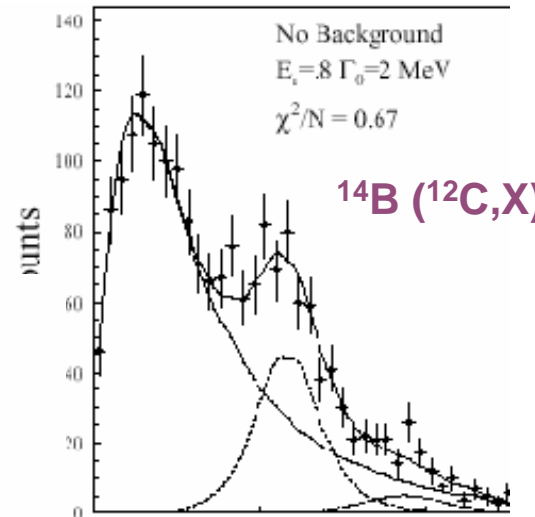
(Korsheninnikov) (1995).



^{12}Be (d,p)



- ^{14}B fragmentation: GANIL (Lecouey, Orr) (2002).

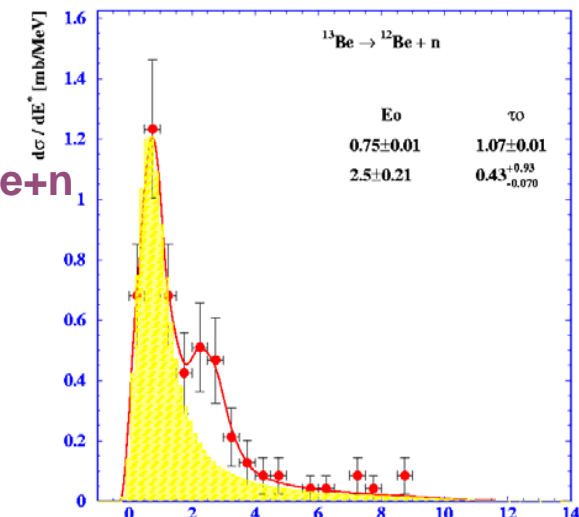


G. Blanchon, A. Bonaccorso
and N. Vinh Mau
Unbound exotic nuclei studied by transfer to the continuum reactions
Nucl. Phys. A739 (2004) 259.

G. Blanchon, A. Bonaccorso,
D. M. Brink, A. Garcia-Camacho
and N. Vinh Mau
Unbound exotic nuclei studied by projectile fragmentation reactions.
nucl-th/0611049 . NPA (2006) in press.

- GSI (U. Datta Pramanik) (2004).

• Unpublished



H. Simon et al. N.P.A734 (2004) 323,
and private communication.

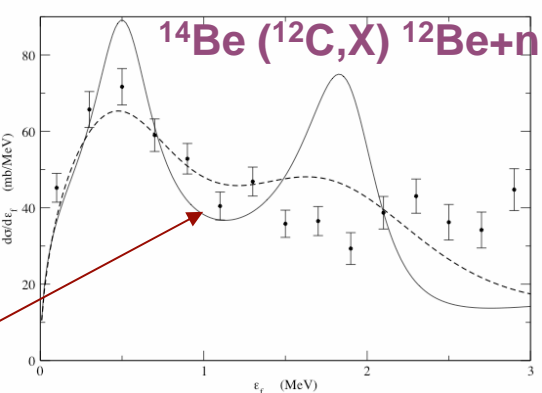


Figure 12: Sum of all transitions from the s initial state with $e_f = -1.85$ MeV (solid line). Experimental points from L. Chulkov et al. [56]. Dashed line is the folding of the calculated spectrum with the experimental resolution curve.

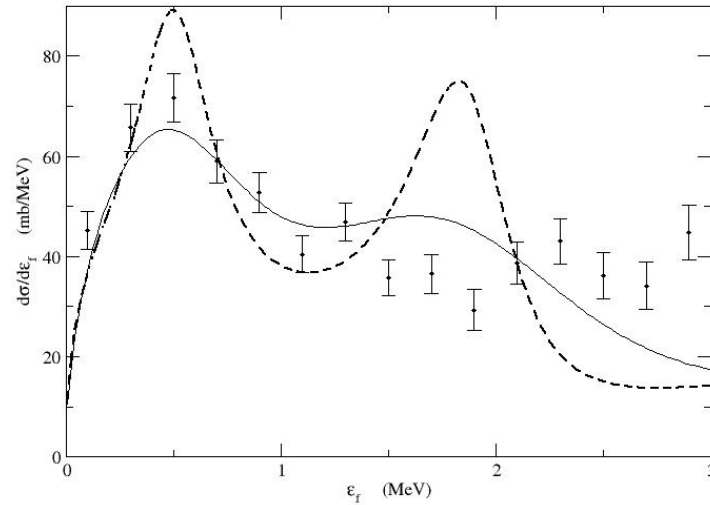


Figure 12: Sum of all transitions from the s initial state with $\varepsilon_f = -1.85$ MeV (solid line). Experimental points from L. Chulkov et al. [56]. Dashed line is the folding of the calculated spectrum with the experimental resolution curve.

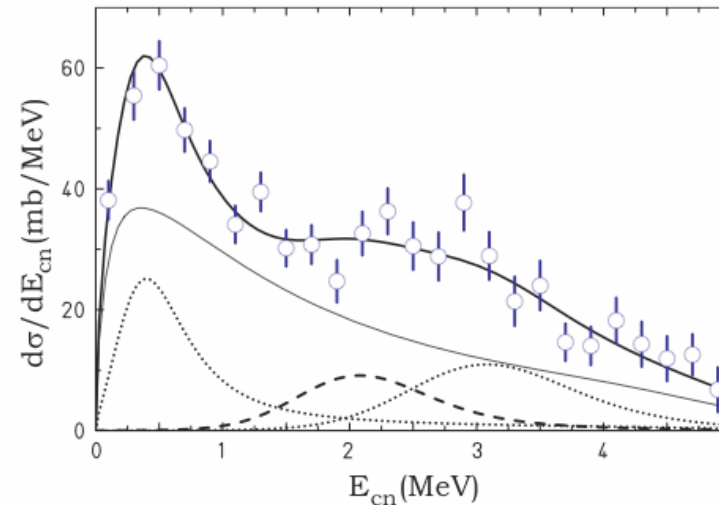


Fig. 10. Decomposition of the distribution of the relative energy between ^{12}Be and a neutron. The thin-solid line corresponds to the $1/2^+$ scattering state, the dashed line describes the contribution from the $5/2^+$ state. Dotted lines display the $1/2^-$ state and its satellite at low energy. The thick-solid line is the sum of the reaction branches

in preparation, private communication.

Systematic investigation of the drip-line nuclei
 ^{11}Li and ^{14}Be and their unbound subsystems
 ^{10}Li and ^{13}Be .

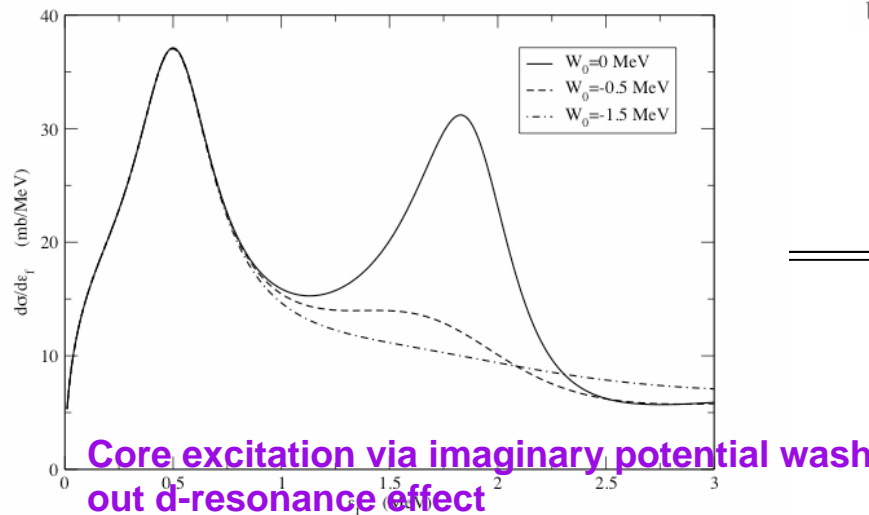


Figure 13: Sum of all transitions from the s initial state with $\varepsilon_f = -1.85$ MeV including core excitation via an imaginary part of the optical potential for the d-resonance only.

H. Simon ^{a,b}, M. Meister ^{a,c}, T. Aumann ^{b,d}, M.J.G. Borge ^e,
 L.V. Chulkov ^{b,f}, Th. W. Elze ^g, H. Emling ^b, C. Forseén ^{h,c},
 H. Geissel ^b, M. Hellström ^b, B. Jonson ^c, J. V. Kratz ^d,
 R. Kulessa ⁱ, Y. Leifels ^b, K. Markenroth ^c, G. Münzenberg ^b,
 F. Nickel ^b, T. Nilsson ^{a,c}, G. Nyman ^c, A. Richter ^a,
 K. Riisager ^j, C. Scheidenberger ^b, G. Schrieder ^a, O. Tengblad ^e
 and M. V. Zhukov ^c

All orders breakup of heavy exotic nuclei

A. García-Camacho et al.,

Nuclear Physics A (2006), doi:10.1016/j.nuclphysa.2006.07.033.

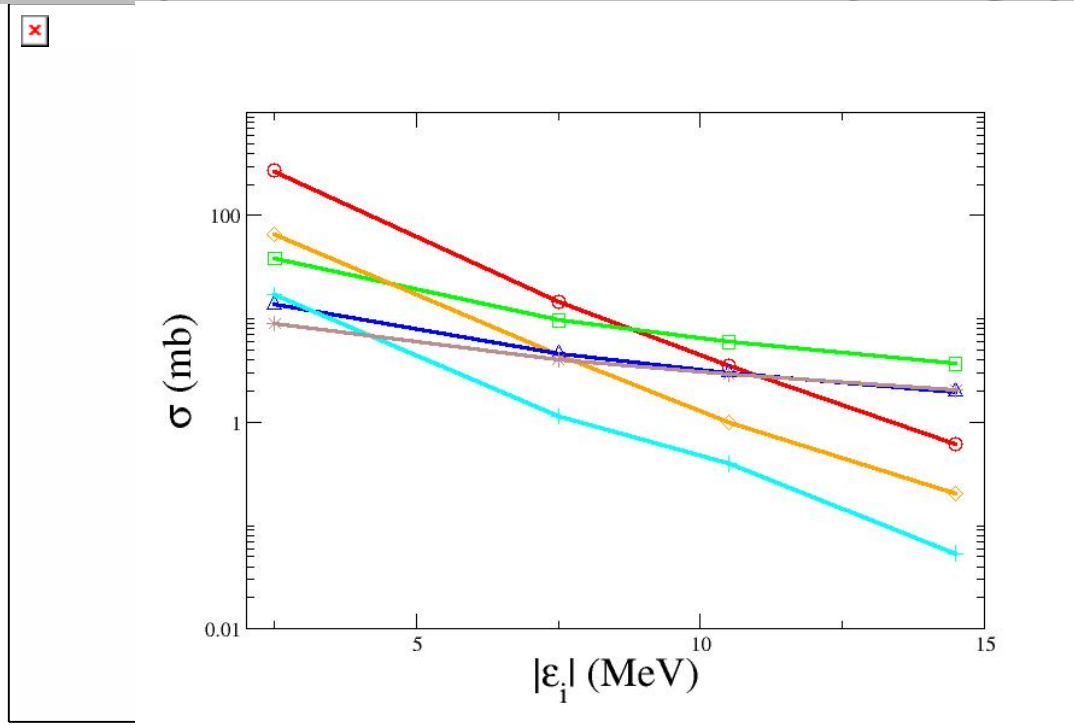


Figure 13: Integrated elastic breakup cross-section for a hypothetical Si beam against Pb at 70 A.MeV as a function of the neutron separation energy. Different initial parameters: circles (squares) are for Coulomb (nuclear) breakup from an initial s-wave; diamonds (triangles) for Coulomb (nuclear) breakup from a d-wave; pluses (stars) for Coulomb (nuclear) breakup from an initial f-wave.

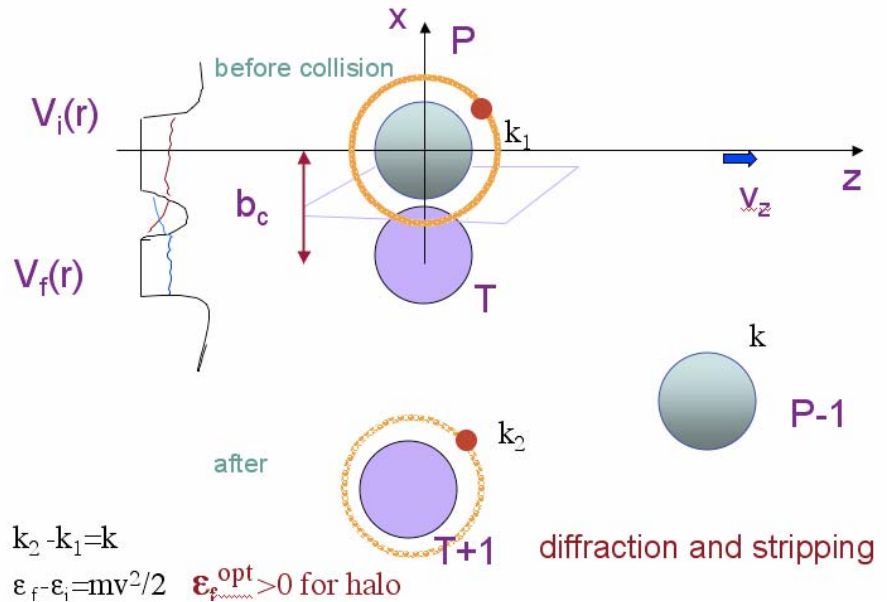
End of

The EURISOL logo consists of the word "EURISOL" in a bold, sans-serif font. Each letter is filled with a different color from a rainbow gradient: purple, red, orange, yellow, green, blue, and purple again. The letters are outlined in black.

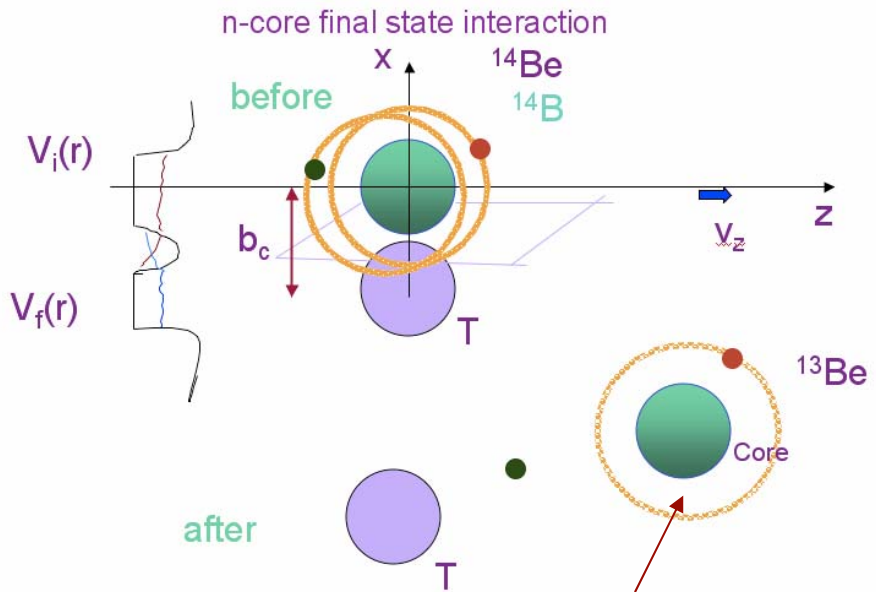
Talk

REACTION MECHANISMS

1. Transfer to the continuum dynamics (knockout)

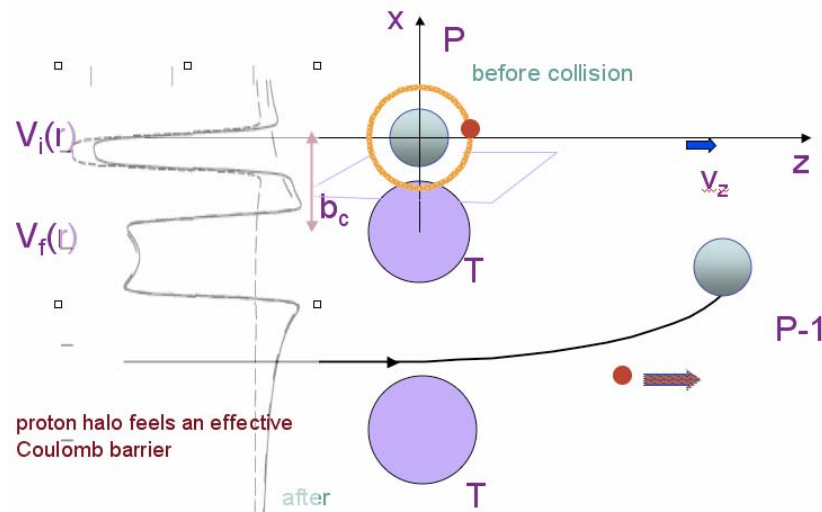


2. Projectile fragmentation



sudden vs
final state interaction

3. Coulomb Breakup : core recoil



Analytical methods for transfer and breakup

Seeking a clear physical interpretation of DWBA (**Brink et al. since 1978 H. Hasan**).

$$\sigma = \int d^2 b_c P_{el}(b_c) P_{tr}(b_c);$$

$$P_{tr} = |A|^2 \longrightarrow A = \frac{1}{i\hbar} \int dt \langle \psi_f(r, t) | V_2 | \psi_i(r - R(t), t) \rangle$$

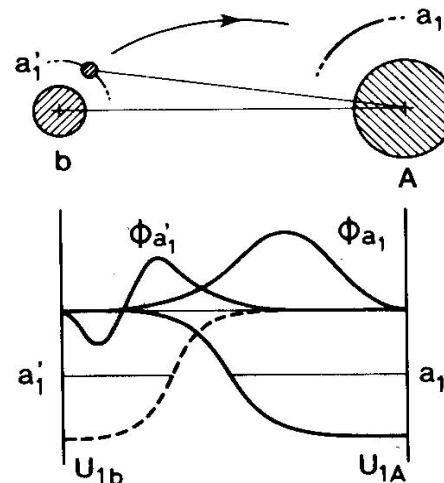
similar to Alder & Winther for Coulomb excitations.

- Transfer between bound states and spin coupling
(L. Lo Monaco, I. Stancu, H. Hashim , G. Piccolo, 1985).
- Transfer to the continuum (1988).
- Coulomb breakup to all orders and coupled to nuclear breakup:
interference effects. (J. Margueron, 2002).
- Full multipole expansion of Coulomb potential, proton breakup
(A. Garcia-Camacho, 2005/2006).
- Projectile fragmentation (G. Blanchon, 2005/06).

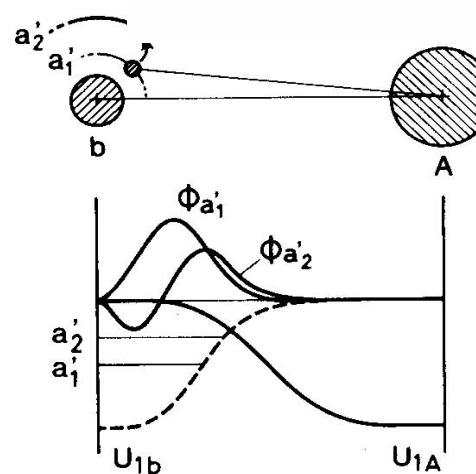
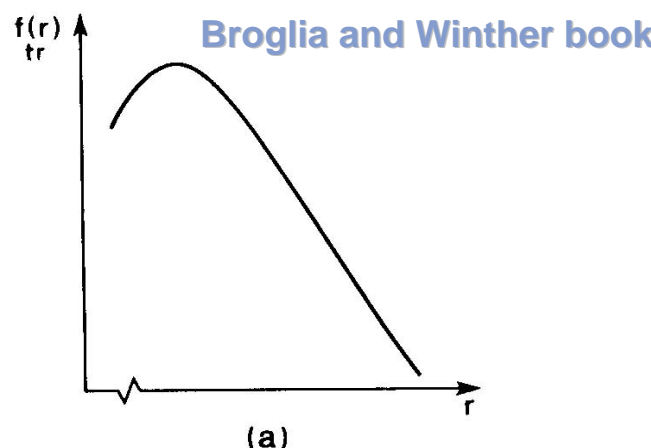
$$\begin{aligned}
 A_{bup} &= \frac{1}{i\hbar} \int_{-\infty}^{\infty} dt \langle \psi_2(t) | V_{nt}(r) | \psi_1(t) \rangle \\
 &\approx \int dk_y \sqrt{k_y^2 + \eta^2} \bar{\psi}_i(d_1, k_y, k_1) \bar{\psi}_f^*(d_2, k_y, k_2)
 \end{aligned}$$

$$A_{fi} = \frac{v_2}{i\hbar v} \int_{-\infty}^{\infty} dz \psi_f^*(b_c, 0, z) \psi_i(b_c, 0, z) e^{iqz}.$$

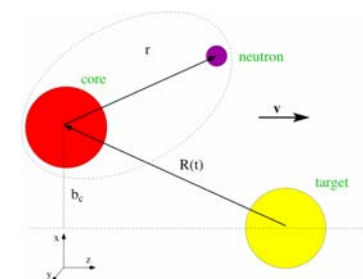
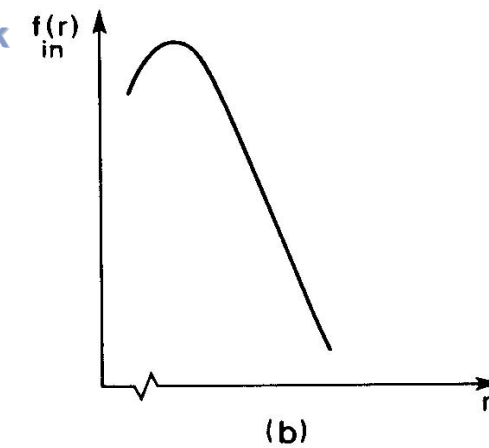
$$A_{fi} = \frac{v_2}{i\hbar v} \int_{-\infty}^{\infty} dz \psi_f^*(b_c, 0, z) \psi_i(b_c, 0, z) e^{iqz}.$$



**TRANSFER
Stripping &
Diffraction
Overlap of
momentum
distribution
(Fourier
transforms)**



**INELASTIC
Diffraction
Fourier transform
of the overlap**



$$A_{fi} = \frac{1}{i\hbar} \int_{-\infty}^{\infty} dt \langle \psi_f(\mathbf{r}, t) | V_2(\mathbf{r} - \mathbf{R}(t)) | \psi_i(\mathbf{r}, t) \rangle,$$

$$\frac{dP_{in}}{d\varepsilon_f} = \frac{2}{\pi} \frac{v_2^2}{\hbar^2 v^2} C_i^2 \frac{m}{\hbar^2 k} \frac{1}{2l_i + 1} \Sigma_{m_i, m_f} |1 - \bar{S}_{m_i, m_f}|^2 |I_{m_i, m_f}|^2,$$

$$\bar{S} = S e^{2i\nu} = e^{2i(\delta+\nu)}$$

$$B_{l_f, l_i} \approx \frac{e^{-2\eta b_c}}{b_c} \quad \text{Transf.}$$

$$\begin{aligned} \frac{d\sigma}{d\varepsilon_f} &\approx \frac{1}{k} \left(\frac{k \cos \delta - \gamma \sin \delta}{\gamma^2 + k^2} \right)^2 \\ &\approx \frac{1}{k} |\sin(\delta + \beta)|^2 \end{aligned}$$

$$I_{l_f, l_i} \approx \frac{e^{-2\gamma b_c}}{b_c^3} \quad \text{Inel.}$$

cf. G. F. Bertsch, K. Hencken and H. Esbensen, Phys. Rev. C57 (1998) 1366.

Differences

- Transfer to the continuum.
- Long range form factor.
- Overlap of momentum distributions
- On shell n-N S-Matrix
- Projectile fragmentation.
- Short range form factor.
- Momentum distribution of overlap
- Off-the-energy-shell n-N S-matrix

Dripline position: from bound nuclei to nuclei unstable by neutron/proton decay.

- Neutron - core potential must be studied in order to understand borromean nuclei.
- ^{11}Li , ^{14}Be and ^{13}Be
- From structure theory point of view:
- $S_{1/2}$ g.s? relevant p and d components ? Core excitation effects?
- From reaction theory point of view:
- i) Scattering with threshold resonances.
- ii) Sudden approximation and one- or two step processes.

Resumee:

^{13}Be has been obtained from:

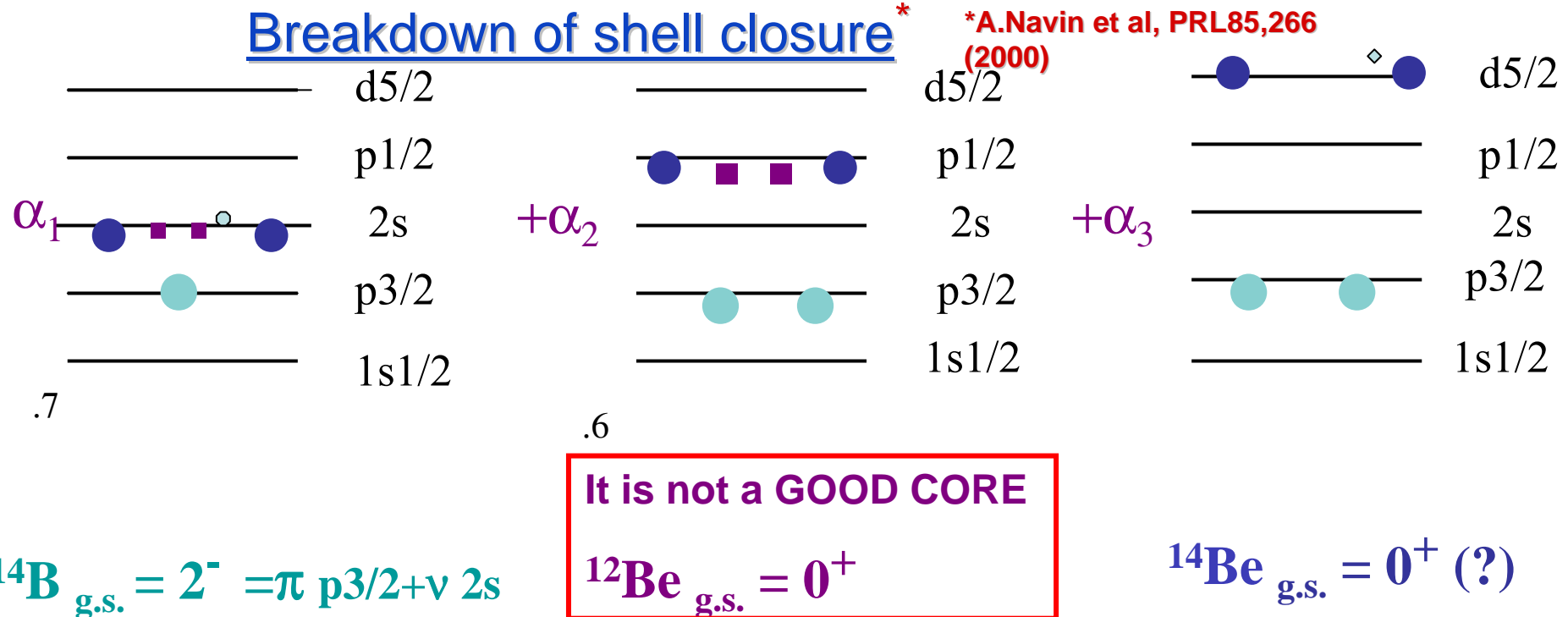
- transfer to the continuum: ^{12}Be (d,p) RIKEN (**Korsheninnikov**) (1995).
- ^{14}B fragmentation: GANIL (**Lecouey**, Orr) (2002).
- GSI (U. Datta Pramanik)(2004).
- ^{14}Be nuclear breakup , GSI (**Simon**), 287AMeV, n-core angular correlations
- ^{14}Be nuclear and Coulomb breakup: GANIL (**K. Jones** thesis, 2000).
- $^{14}\text{C} + ^{11}\text{B}$ multinucleon transfer: (Berlin Group ,1998).
- ^{18}O fragmentation MSU (Thoennessen, 2001) n-core relative velocity spectra.
- ^{14}Be nuclear breakup: RIKEN (Nakamura, Fukuda) (2004).

Transfer to the continuum and projectile fragmentation

Do they convey the same information?...

the same n-core phase shifts?

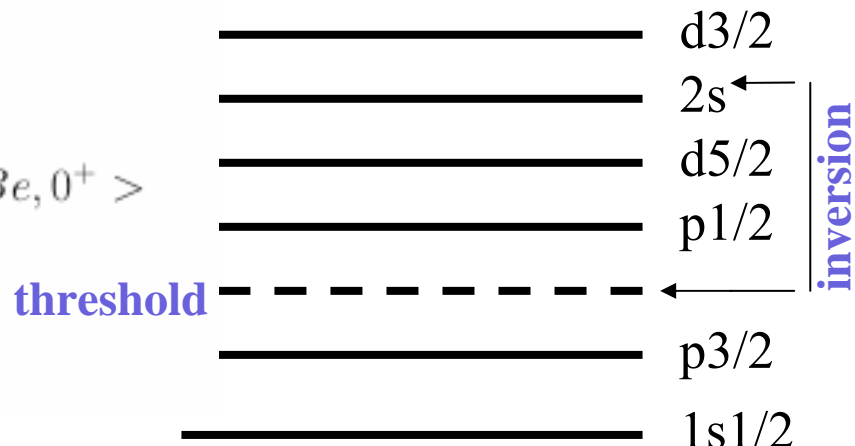
Is the overlap of resonances the same?



$$|^{14}B\rangle = [a_1(p_{3/2}, 2s_{1/2}^\circ) + a_2(p_{3/2}, d_{5/2})] \otimes |^{12}Be, 0^+ \rangle$$

$$|^{14}Be\rangle = [b_1(s_{1/2})^2 + b_2(1p_{1/2})^2 + b_3(1d_{5/2})^2] \otimes |^{12}Be, 0^+ \rangle$$

$$c_3(1d_{5/2})^2] \otimes |^{12}Be^*, 2^+ \rangle$$



Potential corrections due to the particle-vibration coupling (N. Vinh Mau and J. C. Pacheco, NPA607 (1996) 163.

also T. Tarutina, I.J. Thompson, J.A. Tostevin NPA733 (2004) 53)

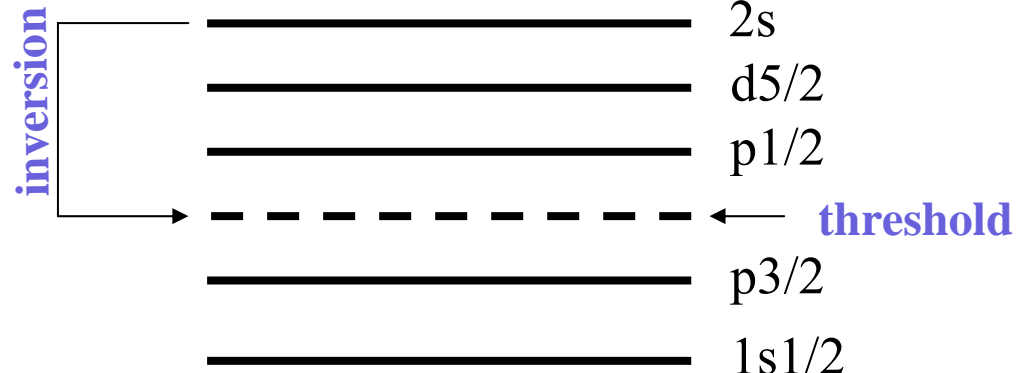
...can be modeled as:

$$U(r) = V_{ws} + V_{so} + \delta V$$

$$\delta V(r) = 16 \alpha e^{(r-R)/a} / (1+e^{(r-R)/a})^4$$

n+¹²Be:

	ε_{res} (MeV)	Γ (MeV)	α (MeV)
1p _{1/2}	0.67	0.28	8.34
1d _{5/2}	2.0	0.40	-2.36



Results

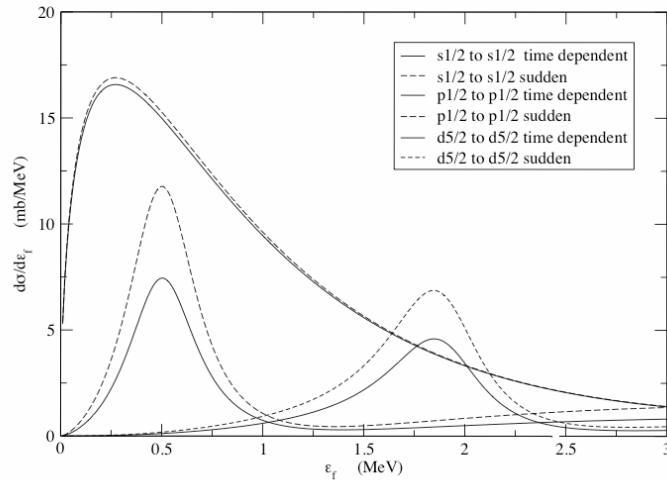


Figure 5: Population of resonances in the $n-^{12}\text{Be}$ relative energy spectrum. Comparison of sudden (dashed line) and non-sudden (solid line) results for an $s \rightarrow s$ transition with peak at 0.25 MeV, $p \rightarrow p$ with peak at 0.5 MeV and $d \rightarrow d$ transition with peak around 2 MeV. See text for details.

sudden → $\mathbf{q=0}$

check of sudden approximation {

- E_{inc} : independent
- ω_{if} : important

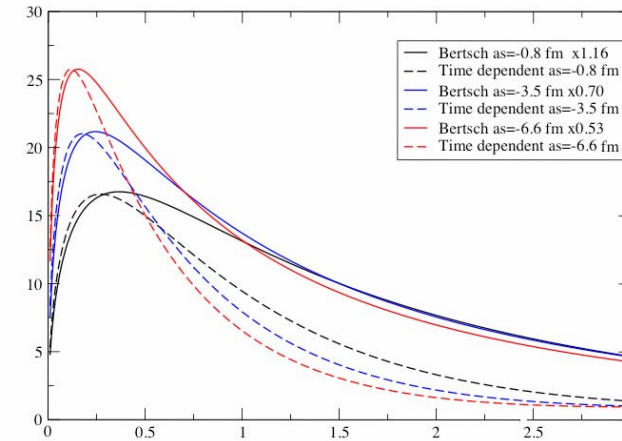


Figure 7: Comparison of time dependent calculation for an s to s transition with results of Eq.(28) using the same optical model phase shifts corresponding to scattering lengths as indicated.

$$\begin{aligned}
 \text{sudden} \rightarrow \frac{d\sigma}{d\varepsilon_f} &\approx \frac{1}{k} \left(\frac{k \cos \delta - \gamma \sin \delta}{\gamma^2 + k^2} \right)^2 \\
 &\approx \frac{1}{k} |\sin(\delta + \beta)|^2
 \end{aligned}$$

Final s-state: continuum vs bound

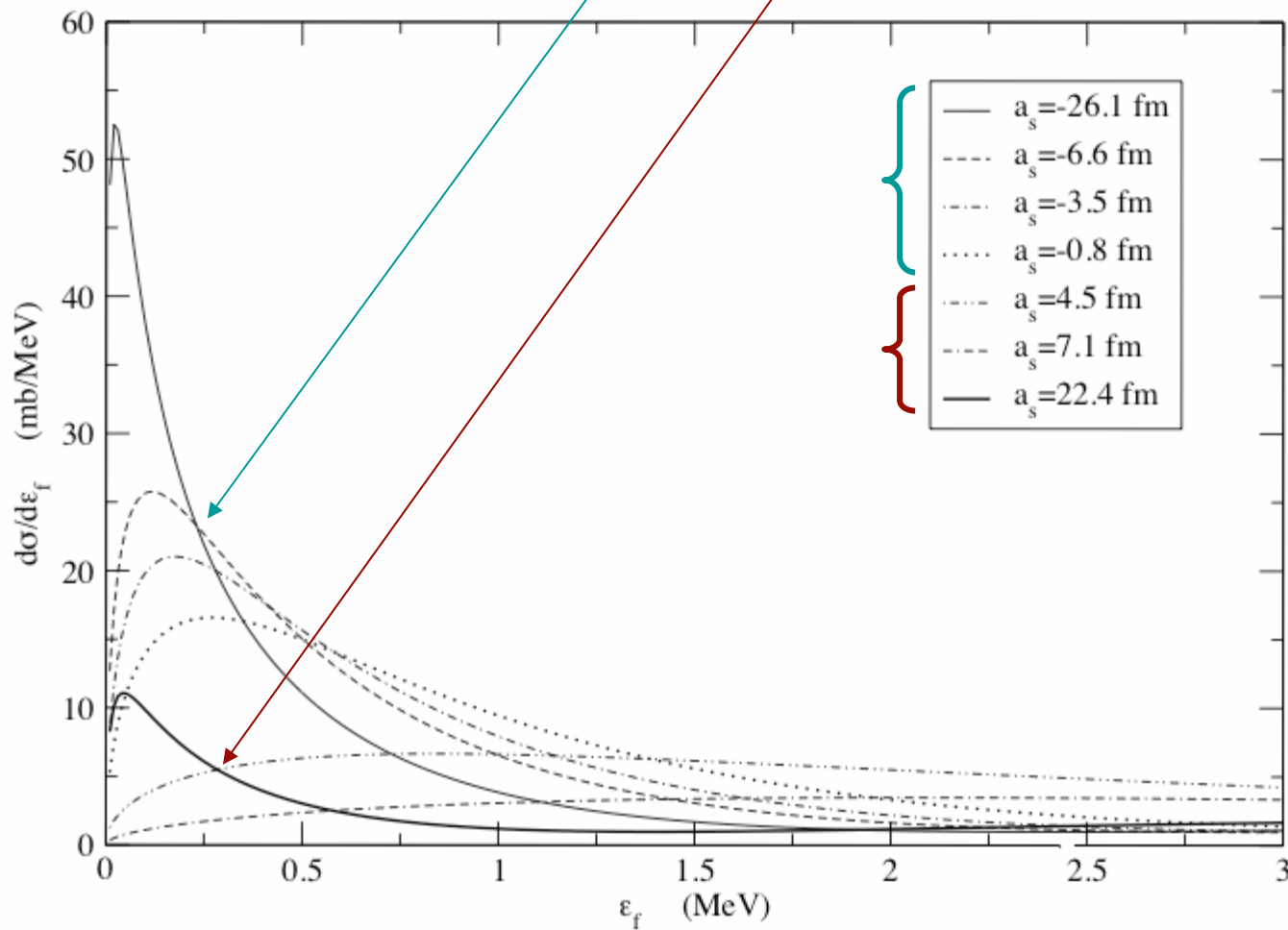


Figure 6: Comparison of results obtained considering a final s-state for the $n-^{12}\text{Be}$ relative energy spectrum with positive and negative scattering lengths. Scattering lengths are given on the figure and their corresponding δV potential strengths in Table 5.

Peak positions of continuum states are not low enough to make accurate predictions by the

effective range theory (1⁰ order)

$$\rightarrow k \cotan \delta = -\frac{1}{a_s} + \frac{1}{2} r_o k^2$$

α (MeV)	a_s (fm)	r_e (fm)	$ \epsilon $ (MeV)
8.0	-0.8	117.0	
4.0	-3.5	17.9	
2.0	-6.6	11.8	
-1.0	-26.1	7.58	
-5.0	22.4	5.9	0.06
-15.0	7.1	3.8	1.34
-35.0	4.5	2.7	6.49

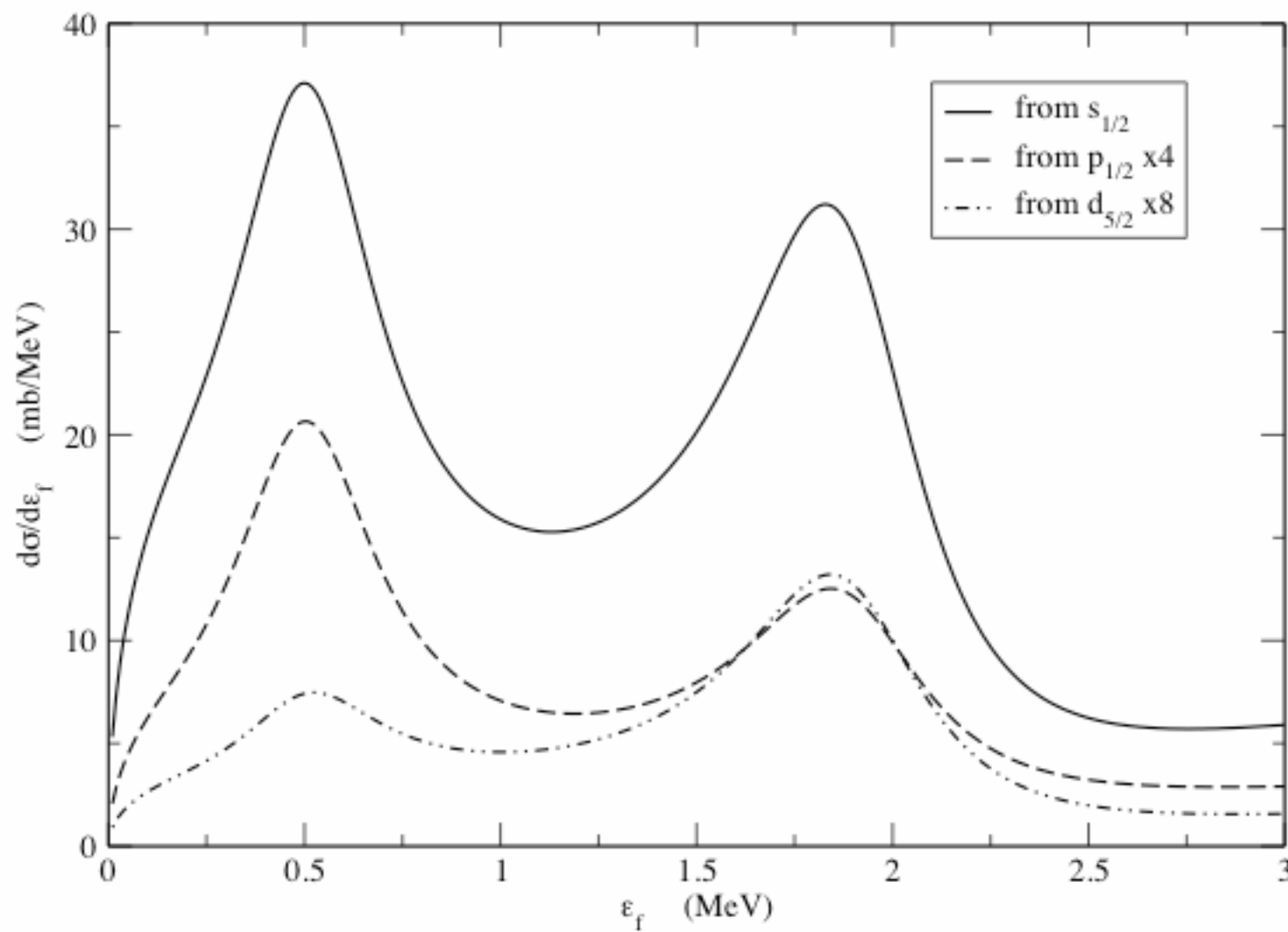


Figure 11: Check of the dependence from the initial state angular momentum. Full curve: sum of transitions from s -initial state. Dashed and dotdashed lines: sum of transitions from p and d -initial states respectively.

Consistent results only if:

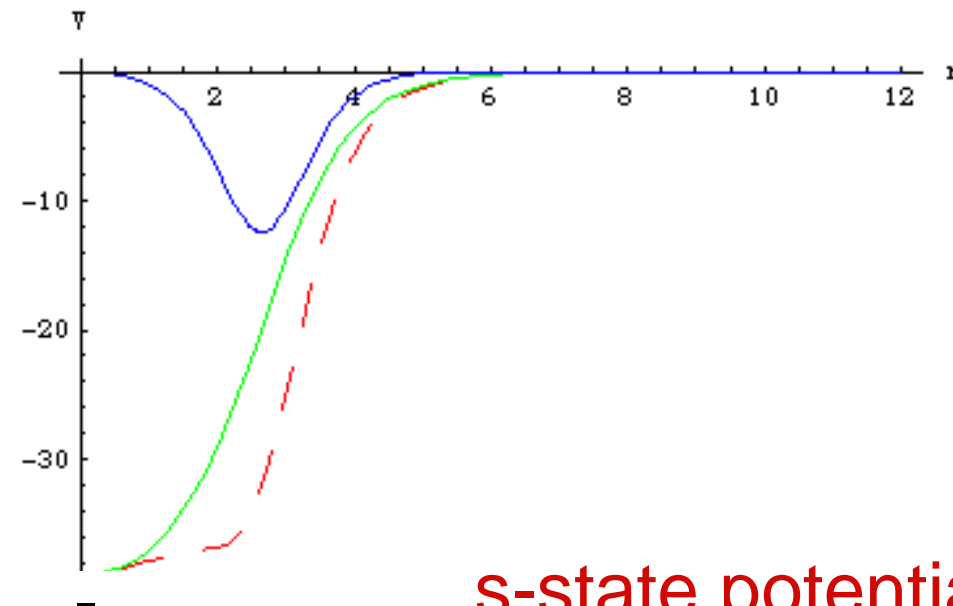
- All bound to continuum transitions are considered (final state effects vs. sudden).
- Correct form factor.
- Optical model phase shifts.
- *Final state interaction effect seems MORE important than sudden effect for not very developed haloes*

$$A_{fi} = \frac{1}{i\hbar} \int_{-\infty}^{\infty} dt dx dy dz \phi_f^*(x, y, z) \phi_i(x, y, z) e^{i\omega t} V_2(x - b_c, y, z - vt),$$

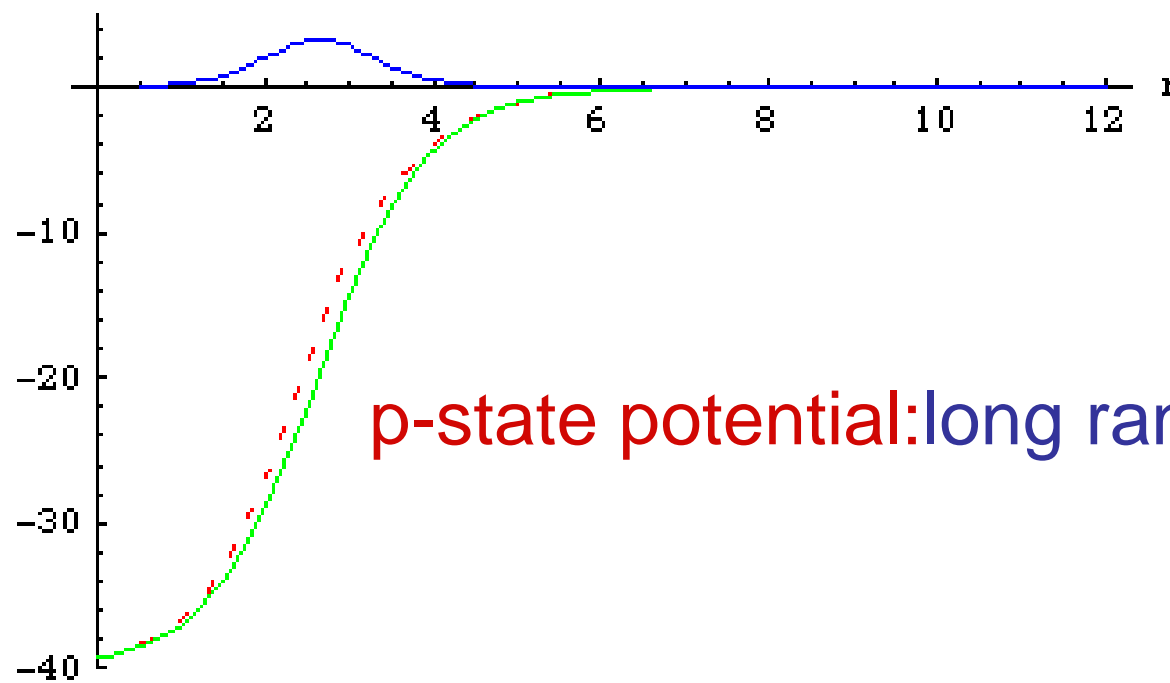
$$V_2(x - b_c, y, q) = \int_{-\infty}^{\infty} dz V_2(x - b_c, y, z) e^{iqz}.$$

Fourier transform of the overlap

$$A_{fi} = \frac{v_2}{i\hbar v} \int_{-\infty}^{\infty} dz \phi_f^*(b_c, 0, z) \phi_i(b_c, 0, z) e^{iqz}.$$



s-state potential:long range added



p-state potential:long range subtracted

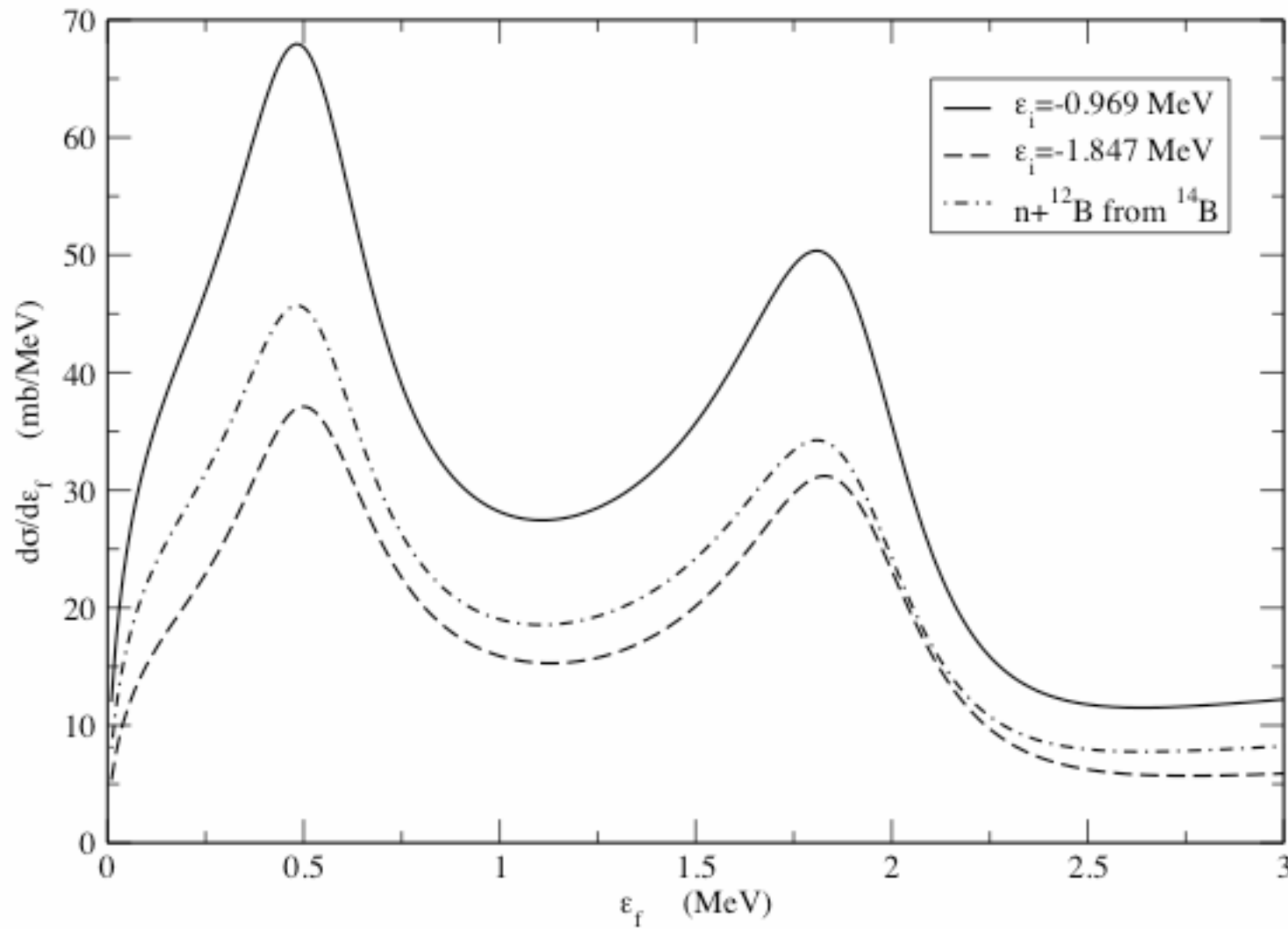


Figure 10: Check of the dependence from the initial binding energy of the sum of transitions from s-initial state. Full curve: $\varepsilon_i = -0.97$ MeV as in ^{14}B ; dashed curve: $\varepsilon_i = -1.85$ MeV as in ^{14}Be [50]. Dotdashed line: sum of transitions from s, p and d-initial states including spectroscopic factors of 0.66, 0.04, 0.30 respectively as in ^{14}B [49] with $\varepsilon_i = -0.97$ MeV.

$$\frac{d\sigma}{d\vec{k}} = \frac{1}{8\pi^3} \frac{mk}{\hbar^2} \int d\vec{b}_c |S_{ct}(b_c)|^2 |g^{nuc} + g^{dir} + g^{rec}|^2.$$

$$g_{fi}(\vec{k}, \vec{b}) = \frac{1}{i\hbar} \int d^3\vec{r} \int dt e^{-i\vec{k}\cdot\vec{r} + i\omega t - i\chi_{eik}(\vec{r}, t)} V(\vec{r}, \vec{R}(t)) \phi_i(\vec{r}),$$

$$g^{nuc} = \int d\vec{r} e^{i\vec{k}\cdot\vec{r}} \phi_i(\vec{r}) \left(e^{i\chi_{nt}(b_v)} - 1 \right).$$

$$g^{dir} = \int d\vec{r} e^{i\vec{k}\cdot\vec{r}} \phi_i(\vec{r}) \left(e^{i\frac{2V_v}{\hbar v} \log \frac{b_v}{R_\perp}} - 1 + \frac{2V_v}{\hbar v} \log \frac{b_v}{R_\perp} + \chi(-\beta_2, V_v) \right),$$

$$g^{rec} = \int d\vec{r} e^{i\vec{k}\cdot\vec{r}} \phi_i(\vec{r}) \left(e^{i\frac{2V_c}{\hbar v} \log \frac{b_c}{R_\perp}} - 1 - \frac{2V_c}{\hbar v} \log \frac{b_c}{R_\perp} + \chi(\beta_1, V_c) \right),$$